HHS Public Access

Author manuscript

Mol Cell. Author manuscript; available in PMC 2020 December 05.

Published in final edited form as:

Mol Cell. 2019 December 05; 76(5): 712–723.e4. doi:10.1016/j.molcel.2019.10.013.

Structural Basis of H2B Ubiquitination-Dependent H3K4 Methylation by COMPASS

Peter L. Hsu[1,2,4], **Hui Shi**[1,2,4], **Calvin Leonen**[3], **Jianming Kang**[3], **Champak Chatterjee**[3,*], **Ning Zheng**[1,2,5,*]

[1]Department of Pharmacology, Box 357280, University of Washington, Seattle, WA 98195, USA

[2]Howard Hughes Medical Institute, University of Washington, Seattle, WA 98195, USA

[3]Department of Chemistry, University of Washington, Seattle, WA 98195, USA

[4]These authors contributed equally

[5]Lead Contact

SUMMARY

The COMPASS (complex of proteins associated with Set1) complex represents the prototype of the SET1/MLL family of methyltransferases that controls gene transcription by H3K4 methylation (H3K4me). Although H2B monoubiquitination (H2Bub) is well known as a prerequisite histone mark for COMPASS activity, how H2Bub activates COMPASS remains unclear. Here, we report the cryoelectron microscopy (cryo-EM) structures of an extended COMPASS catalytic module (CM) bound to the H2Bub and free nucleosome. The COMPASS CM clamps onto the nucleosome disk-face via an extensive interface to capture the flexible H3 N-terminal tail. The interface also sandwiches a critical Set1 arginine-rich motif (ARM) that autoinhibits COMPASS. Unexpectedly, without enhancing COMPASS-nucleosome interaction, H2Bub activates the enzymatic assembly by packing against Swd1 and alleviating the inhibitory effect of the Set1 ARM upon fastening it to the acidic patch. By delineating the spatial configuration of the COMPASS-H2Bub-nucleosome assembly, our studies establish the structural framework for understanding the long-studied H2Bub-H3K4me histone modification crosstalk.

Graphical Abstract

*Correspondence: chatterjee@chem.washington.edu (C.C.), nzheng@uw.edu (N.Z.).

AUTHOR CONTRIBUTIONS

P.L.H. and N.Z. conceived the project. P.L.H. purified all proteins used in this study, with the exception of individual histones. H.S. screened initial cryo-EM grid conditions and collected cryo-EM data, with assistance from P.L.H. H.S. processed the cryo-EM data and generated maps for model building. Model building was conducted by P.L.H., with guidance from N.Z. P.L.H. conducted all binding and methyltransferase assays. C.L. and C.C. prepared large-scale nucleosomes used for structural studies. J.K. and C.C. prepared H2Bub-octamers for uNCP reconstitutions by P.L.H. The manuscript was written by P.L.H. and N.Z., with input from all authors.

SUPPLEMENTAL INFORMATION

Supplemental Information can be found online at https://doi.org/10.1016/j.molcel.2019.10.013.

DECLARATION OF INTERESTS

The authors declare no competing financial interests. N.Z. is a member of the scientific advisory board of Kymera Therapeutics and a co-founder of Coho Therapeutics.

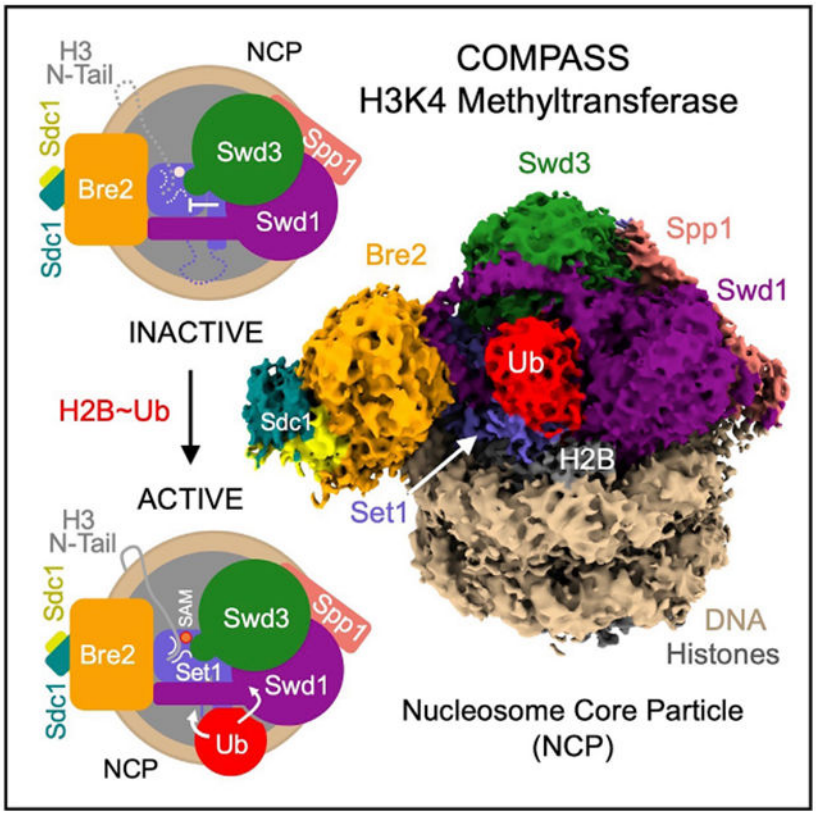

In Brief

The cryo-EM structures of the yeast COMPASS methyltransferase bound to H2Bub and unmodified nucleosomes reveal an arginine-rich motif in the catalytic subunit, whose autoinhibitory effect on the enzymatic complex is overridden by H2B-conjugated ubiquitin. The study sheds light on the mechanism of an evolutionarily conserved crosstalk between two histone modifications.

INTRODUCTION

Methylation of histone H3 at lysine 4 (H3K4me) is an evolutionarily conserved post-translational modification that marks actively transcribed genes and regulates transcription in eukaryotic cells. In humans, H3K4 methylation is catalyzed by the SET1/MLL family of histone methyltransferases, which consists of six family members, MLL1–4, SETD1A, and SETD1B (Shilatifard, 2012). These enzymes use the methyl-donor S-adenosylmethionine (SAM) to mark H3K4 with different degrees of methylation (Ardehali et al., 2011; Denissov et al., 2014; Herz et al., 2012; Hu et al., 2013; Lee et al., 2013; Southall et al., 2009; Wang et al., 2009; Wu et al., 2008).

The catalytic activity of the SET1/MLL enzymes resides in their highly conserved C-terminal SET (Suppressor of variegation, Enhancer of zeste, Trithorax) domains, which are largely inactive on their own (Patel et al., 2009; Shinsky et al., 2014; Southall et al., 2009; Zhang et al., 2015). The SET domains of SET1/MLL methyltransferases must scaffold four

binding partners, collectively known as WRAD (WDR5, RBBP5, ASH2L, and DPY-30), to form an active catalytic module (CM) that imparts both enzymatic activity and product specificity (H3K4me1, H3K4me2, or H3K4me3) (Cao et al., 2010; Dou et al., 2006; Patel et al., 2009; Shinsky et al., 2015). Such a requirement is not only conserved in animals, but also in yeast. In fact, yeast Set1, the founding member of the SET1/MLL family, was initially identified and characterized as part of a large multi-protein complex, known as COMPASS (complex of proteins associated with Set1), which features a similar CM (Halbach et al., 2009; Krogan et al., 2002; Mersman et al., 2012; Miller et al., 2001; Nagy et al., 2002; Roguev et al., 2001). By unveiling the architecture of the CMs of COMPASS and COMPASS-like MLL complexes, recent structural studies have shed light on how WRAD activates their SET domains and, together, governs their product specificity (Hsu et al., 2018; Li et al., 2016; Qu et al., 2018). While these studies have illustrated the structural basis of their catalytic activity, how the SET1/MLL enzymatic complexes respond to regulatory signals remains unclear.

Histone H2B monoubiquitination (H2Bub) is a conserved histone mark, which is associated with actively transcribing genes and regulates a myriad of transcriptional processes (Wang et al., 2017). Interestingly, methylation of H3K4 and H3K79, which are catalyzed by COMPASS and DOT1L, respectively, requires H2Bub (Sun and Allis, 2002). Biochemical reconstitution studies have demonstrated the direct activation of these enzymes by the H2B-conjugated ubiquitin (Ub) (Chatterjee et al., 2010; Holt et al., 2015; Kim et al., 2013; McGinty et al., 2008). Despite recent structural studies of H2Bub-dependent H3K79 methylation by DOTL1 (Anderson et al., 2019; Valencia-Sánchez et al., 2019; Worden et al., 2019), how H2Bub activates the multi-subunit COMPASS assembly remains a mystery. Here, we report the cryoelectron microscopy (cryo-EM) structures of an extended CM (eCM) of yeast COMPASS bound to the H2Bub modified and unmodified nucleosome. Our results not only reveal how COMPASS recognizes its nucleosomal substrate but also shed light on how H2Bub allosterically activates the autoinhibited methyltransferase complex.

RESULTS AND DISCUSSION

Reconstitution of H2Bub-Dependent COMPASS Activity

To gain insight into how the catalytic activity of COMPASS is regulated by H2Bub, we first co-expressed and purified the intact eight-subunit *K. lactis* COMPASS and assembled nucleosome core particles (NCPs) containing Ub-modified H2B (uNCPs) (Figure S1A). We and others have previously showed that the five-subunit COMPASS CM complex, which consists of the SET domain of Set1 and the four WRAD subunits (Swd3, Swd1, Bre2, and Sdc1) (Figure 1A), possesses robust activity in methylating H3K4 with unmodified nucleosomes (Hsu et al., 2018; Kim et al., 2013). In contrast, the intact COMPASS exhibited little to no activity against unmodified nucleosomes (Figure 1B). Remarkably, when presented with ubiquitinated nucleosomes, the full COMPASS complex showed robust activity of methylating H3K4 to all three methylation states, which is consistent with its H2Bub-dependent activity in the cell. The lack of enzymatic activity in intact COMPASS toward unmodified nucleosomes suggests that the enzymatic complex is somehow inhibited and might not be able to bind the nucleosomal substrate. To our surprise, COMPASS bound

nucleosomes almost equally well as the isolated five-subunit CM (Figures 1C and S1B). These results suggest that nucleosome binding by COMPASS is necessary, but not sufficient, for the enzymatic complex to methylate H3K4.

With a chromatin substrate, a six-subunit extended CM complex (eCM), which includes the nSET domain of Set1 and the Spp1 subunit (Figure 1A), has been previously reported to be largely inactive and represent the minimal core complex with H2Bub-dependent activities (Kim et al., 2013). With the nucleosome substrate, we observed the same stimulating effect of H2Bub on the purified COMPASS eCM (Figure 1D, lane 2 versus 4). By contrast, the activity of the COMPASS CM was only slightly enhanced by H2Bub (Figure 1D, lane 1 versus 3). Importantly, the COMPASS eCM bound nucleosomes just as well as the intact COMPASS and the CM complexes in the gel shift assay (Figures 1C, 1E, and S1B). It also took the same amount of the COMPASS eCM to shift the NCP in comparison to the uNCP (Figure 1F versus Figure 1E). Together, these results support the notion that the nSET/Spp1 module contains an element that inhibits the intrinsic methyltransferase activity of the CM and confers H2Bub sensitivity to COMPASS. Furthermore, the Ub moiety conjugated to H2B (H2B~Ub) does not increase the substrate-binding affinity of the eCM subcomplex. Instead, it activates the enzyme assembly most likely by reversing the inhibiting effect of the structural element present in the COMPASS eCM outside the CM.

Overall Structure of the COMPASS-uNCP Complex

To reveal the structural basis of H2Bub-dependent H3K4 methylation by COMPASS, we prepared a glutaraldehyde cross-linked sample of the COMPASS eCM-uNCP complex and determined its structure by single-particle cryo-EM to an average resolution of 3.5 Å (Figures 2 and S2; Table S1). As readily visualized in 2D class averages, the COMPASS eCM can bind to both sides of uNCP, forming a complex at a 2:1 ratio. To obtain a high-resolution map, we performed masked global 3D classification, followed by masked 3D refinement, focusing on the 1:1 enzyme-substrate subcomplex (Figure S2). The final map allowed us to unambiguously dock and rebuild models of the nucleosome and most subunits of the COMPASS eCM assembly (Figure S3). For comparison, we also determined the 3.7 Å resolution cryo-EM structure of the COMPASS eCM bound to an unmodified nucleosome. This Ub-free structure reveals a similar overall architecture with discernable local differences (e.g., Figure S3C versus Figure S3D), which will be highlighted after the description of the COMPASS eCM-uNCP structure.

The COMPASS eCM recognizes two distinct parts of its nucleosomal substrate, the surface of the well-ordered NCP disk body and the distal end of the flexible histone H3 N-terminal tail. Upon binding to the nucleosome, the enzymatic complex partitions H2B~Ub and the histone H3 N-terminal tail on its two separate sides (Figure 2B). The COMPASS eCM spans across the entire disk face of the nucleosome and uses four out of six subunits to make direct contacts with all histones and nucleosomal DNA (Figure S4A). Only Swd3 and Sdc1 are isolated from the interface, in support of their roles as structural subunits of the COMPASS assembly. The COMPASS eCM buries a total of ~3,000 $Å^2$ surface area on the nucleosome, consistent with the strong association between the two complexes.

Similar to its central location in the isolated COMPASS eCM, the Set1 SET domain is positioned at the center of the COMPASS eCM-uNCP interface in close proximity to Ub (Figure 2). We were able to observe clear densities for both the SAM cofactor, as well as the entire tip of the H3 N-terminal tail (amino acid 1–8) at the active site of the SET domain (Figure S3C), suggesting that the COMPASS eCM was crosslinked and captured in its pre-reaction state. The remainder of the H3 tail ranging from amino acid 9 to 37 is invisible in our maps, likely due to its intrinsic flexibility. The H3K4 peptide can only weakly bind to the SET1/MLL enzymatic complex with an affinity of ~100 μM (Zhang et al., 2015). The overall bipartite binding mode of the COMPASS eCM to the nucleosome not only underlines the ability of the Set1 catalytic domain to differentiate H3K4 from other histone lysine residues but also accentuates the contribution made by the interactions between COMPASS and nucleosome disk body to target site engagement.

Upon conjugation to H2B, Ub uses its canonical Ile44 hydrophobic patch as well as its C-terminal tail to pack against Swd1. Meanwhile, H2B~Ub also interacts with a long Set1 α-helix adopted by an arginine-rich motif (ARM) immediately preceding and outside the SET domain in sequence (Figure 2A). Unlike many other chromatin-binding proteins (Figure S4; McGinty and Tan, 2016), the COMPASS CM subunits shared among all SET1/MLL enzymes do not interact with, but instead arch over, the H2A-H2B acidic patch (Figure 2A). Interestingly, the space between is occupied by the Set1 ARM helix, which is evolutionarily conserved but unique to fungi Set1 proteins and their mammalian orthologs, SETD1A and SETD1B, whose enzymatic activities are H2Bub dependent. The Set1 ARM helix stands out as the hallmark of the COMPASS eCM-uNCP assembly by not only anchoring its N-terminal half right next to the SET-domain-nucleosome interface but also employing its C-terminal half to directly contact H2B~Ub.

Bre2 and Spp1 Bind Nucleosomal DNA

Previous studies have suggested that protein-nucleic-acid interactions are critical for COMPASS and COMPASS-like complexes to recognize and methylate substrates (Chen et al., 2011; Trésaugues et al., 2006). The COMPASS eCM-uNCP complex structure reveals multiple DNA contacts made by Spp1 (CFP1 in humans) and the WRAD subunit Bre2 at the two extreme ends of the interface (Figure 3A). Although clear densities were observed for the majority of the nucleosome-COMPASS interface, the local resolution for Spp1 and Bre2-Sdc1, which are at the periphery of the complex, was not high enough for manual model building (Figure S3A). Instead, we fit a homology model of the central coiled-coil region of *K. lactis* Spp1 derived from the structure of its *S. cerevisiae* ortholog to the map (Qu et al., 2018). We observed discernable densities contacting the major groove of nucleosomal DNA that corresponds to a region missing in *S. cerevisiae* Spp1 (Figure 3B). This Spp1 region sits at the junction between the two long a helices and contains a series of positively charged residues that is mostly disordered in the absence of the nucleosomal substrate but likely involved in engaging DNA (Figure 3C).

Bre2 mirrors the action of Spp1 by interacting with DNA at the opposite end of the nucleosome (Figure 3A). As previously revealed, Bre2 contains a non-canonical SPRY domain, which is characterized by a twisted auxiliary β sheet harboring a cluster of highly

conserved but solvent-exposed residues (Hsu et al., 2018). At the COMPASS-DNA interface, Bre2 embraces the phosphate backbone of nucleosomal DNA using the edge of its auxiliary β sheet (Figure 3D). To assess the significance of this interface, we purified COMPASS CM with two sets of Bre2 mutations, focusing on two highly conserved lysine residues on the surface of the auxiliary β sheet that are in close proximity to the phosphate backbone of DNA (Figure 3D, right panel). Compared to the wild-type protein, mutation of Bre2 Lys49 showed a minor effect on the methyltransferase activity, whereas a Bre2 double mutant, Ile251Ala and Lys254Ala (IK → AA), severely compromised the production of H3K4 in all three methylation states (Figure 3E). As expected, this loss of enzymatic activity is attributable to the disruption of nucleosome binding by the dual mutation as assessed by gel shift assays (Figures S1B and S1C). Taken together, these data suggest that DNA binding by Bre2 is critical for the recruitment and activity of COMPASS on nucleosomes.

Swd1 Contacts All Four Histones and Nucleosomal DNA

Swd1 plays a critical role in organizing the COMPASS eCM by interacting with almost every subunit except Sdc1 (Halbach et al., 2009; Hsu et al., 2018; Qu et al., 2018). This functional importance of Swd1 is further magnified by the COMPASS-uNCP structure, in which Swd1 closely interacts with all four core histones, nucleosomal DNA, and Ub. Using the edge of its β-propeller domain and several loop regions, Swd1 docks to the nucleosome disk at a pronounced three-helix cleft formed by the last two helices of H2B (α3 and αC), the second helix of H2A (α2), and DNA (Figures 4A and 4B). As a canonical WD40-repeat-containing protein (Sprague et al., 2000), Swd1 utilizes the conserved loop connecting the “D” strand of blade 5 and the “A” strand of blade 6 (5D-6A loop), as well as the solvent exposed “D” strand of blade 6 to cradle the long C-terminal αC helix of H2B (Figures 4B and 4C). Meanwhile, the tip of the Swd1 5D-6A loop is deeply inserted into the three-helix cleft. Two consecutive Swd1 isoleucine residues, Ile271 and Ile272, interact with a hydrophobic patch formed around H2B Val115 and H2A Tyr50. The interface is enhanced by two nearby invariant Swd1 residues, Asn273 and Arg274, which make a hydrogen bond with H2B Gln96 and a salt bridge with the DNA backbone, respectively (Figures 4D and 4E).

The importance of the conserved 5D-6A loop of Swd1 in locking COMPASS to nucleosomes is underscored by alanine substitutions in this loop. Mutation of its two central hydrophobic residues, Ile271A/Ile272A (II→AA), effectively abolishes H3K4 di- and tri-methylation by the COMPASS CM (Figure 4F). Alanine replacement of all four residues in the loop (IINR→A4) reduces activity of the COMPASS CM to near-background levels for all three methylation states. Importantly, the tetra mutant significantly weakens the binding of the COMPASS CM to nucleosomes, indicating that Swd1 is on par with Bre2 in promoting nucleosomal substrate recognition by the histone methyltransferase complex (Figure S1D).

Binding of the Set1 Catalytic Domain to H2A

The Set1 catalytic domain represents the heart of the COMPASS CM. It is held by a highly conservedWD40 repeat proximal (WDRP) region of Swd1 and is sandwiched between Bre2 and the two CM β-propeller subunits, Swd1 and Swd3 (Figure 2). Superposition analysis

suggests that we have captured the SET domain in a closed conformation that is conducive for catalysis (Figure S5A). In the COMPASS eCM-uNCP structure, the Set1 SET domain is placed at the center of the enzyme-substrate assembly, directly packing against the α2 helix of H2A through a marked interface (Figure 5A). Upon engaging the nucleosome, the N-terminal α-helix of the SET domain unravels into a more linear configuration (Figure 5B and S5B), which enables Lys855 and Arg856 to interact with three H2A residues, Glu64, Asn68, and Asp72, on its α2 helix (Figure 5C). The Set1-H2A interaction is further bolstered by a quintet of hydrophobic Set1 residues, Leu853, Met883, Ile948, Val950, and Val957, which are presented by the β sheet of the SET-N/C subdomain. Together, these residues wrap around the C-terminal tip of the H2A α2 helix and bury H2A Arg71 that is neutralized by the nearby H2B Asp52 residue (Figure 5D). Noticeably, these hydrophobic residues are not only conserved across all Set1 orthologs but also found in all the SET domains of the expanded SET1/MLL family in mammals (Figure S5C). The binding mode of the catalytic SET domain to H2A, therefore, might be common to all SET1/MLL enzymatic complexes.

A previous systematic alanine scanning analysis of all four core histones in yeast has identified four histone H2A residues whose mutations impaired H3K4 di- and trimethylation *in vivo* (Nakanishi et al., 2008). Strikingly, three of these residues are localized at the SET-domain-H2A interface and perfectly match to the three H2A α2 helix amino acids, Glu64, Asn68, and Asp72, that directly interact with the Set1 SET domain (Figure 5C). Proper packing of the Set1 catalytic domain against histone H2A, thus, is critical for COMPASS to maintain its catalytic competency in the context of the nucleosome.

The Ub-COMPASS Interface

The H2B-conjugated Ub moiety makes close interactions with the nucleosome-bound COMPASS eCM via multiple interfaces. Its β-grasp fold not only snugly fits into a concave surface presented by several spatially conglomerated Swd1 structural elements but also packs against a platform formed by the Set1 sequence immediately preceding the catalytic domain (Figures 2 and 6A). As seen in many Ub-protein interfaces (Winget and Mayor, 2010), H2B~Ub uses its Ile44-Val70-Leu8 hydrophobic patch to adhere to a hydrophobic surface formed among Phe10 and Leu13 of the Swd1 N-terminal extension and Val409 of the Swd1 C-terminal tail (Figure 6B). This hydrophobic interface is stabilized on both sides by two nearby positively charged Ub residues, Lys48 and Arg42, which form a salt bridge with Glu15 and Glu405 of Swd1, respectively. The H2B~Ub-Swd1 interface is further extended into the Ub tail, whose two arginine residues, Arg72 and Arg74, cling to the Swd1 β-propeller via additional polar interactions. Overall, a continuous surface area of H2B~Ub that spans ~30 Å is exclusively recognized by Swd1 at this interface, suggesting that the same interactions could take place between H2B~Ub and other SET1/MLL enzymatic complexes.

In addition to the Ile44-centered hydrophobic patch, H2B~Ub also engages with COMPASS via its Ile36 site situated at a separate location of the β-grasp fold (Winget and Mayor, 2010). Upon unraveling, the N-terminal α-helix of the SET domain and its preceding sequence adopt a highly coiled structure, which inserts a loop into the H2B~Ub pocket

demarcated by Ile36, the β1-β2 loop, and the Ub tail (Figure 6C). Within this pocket, Leu847 of Set1 packs against Leu71 and Ile36 of H2B~Ub, while its three preceding residues, Glu844, Ser845, and Asp846, make multiple polar interactions with the β1 -β2 loop of Ub on the opposite side. Moreover, the Swd1 WDRP loop joins in at this interface by stabilizing the Ub Lys11 residue with two negatively charged residues. Strikingly, both Leu71 and Leu73 have been previously identified by an alanine scan of Ub as essential for H2Bub-dependent H3K4 methylation (Holt et al., 2015), indicating that the interface formed between Ub and the unraveled SET N terminus is critical for productive catalytic activation. Furthermore, the majority of the Set1 residues at this three-molecule junction are variable in mammalian Set1 paralogs, MLL1–MLL4, suggesting that this Set1-H2B~Ub interface is most likely unique to fungi Set1 and its mammalian SETD1A and SETD1B orthologs. In fact, this Set1 -specific property is manifested by the further upstream ARM helix of the methyltransferase, which is only found in Set1 orthologs.

Docking of the Set1 ARM Helix to Acidic Patch

Previous studies have identified an ARM flanked by the Set1 nSET and SET domains that plays a critical role in mediating H2Bub-dependent H3K4 methylation by the COMPASS eCM (Kim et al., 2013; Figure 7A). This Set1 motif contains three invariant arginine residues conserved from yeast to humans. Although the Set1 ARM is completely disordered in the free COMPASS eCM structure (Qu et al., 2018), it becomes buried at the COMPASS-uNCP interface and folds into a long α-helix that is directly connected to N terminus of the SET domain.

In the COMPASS-uNCP complex, the Set1 ARM helix runs through the tunnel formed between the COMPASS eCM and the nucleosome disk body and is firmly locked down to the nucleosomal acidic patch (Figure 7B; McGinty and Tan, 2016). At the bottom side of the Set1 ARM helix, two out of the three strictly conserved arginine residues, Arg824 and Arg828, each make multivalent polar interactions with a distinct pair of negatively charged histone acidic patch residues (Figure 7C). They are joined by an upstream arginine residue, Arg821, and four H2A residues, Tyr57, Leu65, Asp90, and Glu92, which further augment the complementary interface. Next to the acidic patch, the Set1 ARM helix is held by the H2B αC helix, which employs two polar residues, Ser112 and Lys116, to form a hydrogen bond with Arg829 and Gln832 of Set1, respectively (Figure 7D). The Set1 ARM helix is further secured by its two hydrophobic residues, Leu822 and Val825, which interact with His109 of H2A through van der Waals packing.

A subset of the H2A-H2B residues interacting with the Set1 ARM helix have also been previously identified in the systematic alanine scanning analysis of histone residues that are required for proper H2Bub-mediated H3K4 methylation (Nakanishi et al., 2008). Specifically, alanine substitution of the H2B resides equivalent to His109 and Lys116, as well as Glu64 and Leu65 of H2A all negatively impacted H3K4 di- and trimethylation *in vivo* (Figures 7C and 7D). These previously published results not only validate the specific Set1 ARM-H2A-H2B interface revealed in the COMPASS eCM-uNCP structure but also echo the loss of function of the Set1 ARM in supporting H2Bub-dependent activity of the COMPASS eCM due to Arg→Ala mutations (Kim et al., 2013).

Effects of H2B~Ub on Set1

Upon anchoring at the nucleosomal acidic patch, the Set1 ARM helix also interfaces with and, thereby, bridges two central components of the COMPASS eCM-uNCP complex, the Set1 catalytic SET domain and H2B~Ub. At one end, the N-terminal half of the Set1 ARM helix buttresses the Set1 catalytic domain that rests on the H2A α2 helix (Figures 5A and 7B). At the other end, the C-terminal half of the same helix presents two hydrophobic and an arginine residue, Phe830, Ile834, and Arg837, to hold onto the highly coiled N-terminal sequence of the SET domain. Together, they give rise to a platform that binds to both the Ile36 site and the C-terminal tail of Ub (Figure 7E).

The central and strategic location of the Set1 ARM helix in the COMPASS eCM-uNCP structure and its crucial role in mediating H2Bub-dependent H3K4 methylation by COMPASS strongly suggests that it is a key factor that sensitizes COMPASS to H2Bub. To better understand the nature the H2Bub-H3K4me crosstalk, we determined the cryo-EM structure of the COMPASS eCM bound to the unmodified NCP (Figure S6) and compared it with the Ub-conjugated form of the nucleosome. In the absence of H2B~Ub, the COMPASS eCM docks to the nucleosome in an overall similar manner as it does to uNCP (Figure S7A). However, the density corresponding to the C-terminal half of the Set1 ARM helix and the N-terminal region of the SET domain is entirely missing (Figure 7F). By contrast, we were able to locate the density for the N-terminal half of the helix, which occupies the acidic patch. This result corroborates the idea that the Set1 ARM helix might be the missing structural element of the COMPASS eCM, which inhibits the enzymatic assembly upon binding to the nucleosome and is overcome by H2B~Ub for enzyme activation.

To validate this hypothesis, we first designed and prepared a COMPASS CM plus (CM+) complex by extending the Set1 SET domain with an extra ~30 amino acids at the N terminus, which excludes the majority of the nSET domain except the ARM. Strikingly, the activity of the COMPASS CM+ was similarly suppressed, like the COMPASS eCM, against naked nucleosome (Figure 7G). In a reaction against uNCPs as substrates, its activity was stimulated to an almost equal extent as the COMPASS eCM, indicating that the evolutionarily conserved Set1 ARM is indeed responsible for coupling H2Bub to enzyme activation (Figure 7G).

In company with the changes at the C-terminal half of the Set1 ARM helix, a profound difference between the uNCP- and NCP-bound COMPASS eCM structures can be found at the catalytic cleft of the Set1 SET domain. Despite the comparable resolution of the two structures, only three residues centered at the H3K4 methylation site show detectable density in the NCP-bound COMPASS structure, whereas all eight N-terminal residues of H3 can be clearly traced for the uNCP-bound form of the enzymatic complex (Figure 7H; Figure S3C versus Figure S3D). By superimposing the nucleosomal portion of the two structures, we also detected a small but considerable degree of global structural changes within the Set1 catalytic domain, which narrow the catalytic cleft without impacting to the position of the SAM cofactor (Figures S7C and S7D). As a whole, the structural differences between the two structures might reflect the impact of H2B~Ub on the dynamic topology of the Set1 catalytic domain, which has been proposed to dictate enzymatic activity (Hsu et al., 2018; Li

et al., 2016; Worden and Wolberger, 2019). We speculate that such an effect might be allosterically transduced through both the Ub-Swd1 and Ub-Set1 interfaces (Figure S7E).

Conclusions

The cryo-EM structure of the COMPASS eCM bound to nucleosome reveals a proximity-enhanced substrate capture mechanism, in which the multisubunit histone methyltransferase attaches itself to the nucleosome body to enable its catalytic subunit to catch the flexible N-terminal tail of H3 bearing the H3K4 methylation site. This substrate engagement mechanism is distinct from many other chromatin modifying enzymes, such as Ring1b-Bmi1-UbcH5c, SAGA-DUB, and DOT1L, which use the histone surface to precisely position their catalytic center in the immediate vicinity of their target sites (Figure S4; Anderson et al., 2019; Jang et al., 2019; McGinty et al., 2014; Morgan et al., 2016; Valencia-Sánchez et al., 2019; Worden et al., 2019).

Binding of COMPASS to the nucleosome disk body not only serves the purpose of substrate recognition but also renders the enzymatic complex susceptible for regulation. The COMPASS eCM-NCP complex is characterized by both extensive interactions among the subunits of the methyltransferase assembly and multiple interfaces made by four out of the six subunits with the nucleosomal disk. These contacts predict that local structural changes and spatial readjustments can propagate through the complex and affect the catalytic activity of the methyltransferase catalytic domain. Specifically, binding of COMPASS to the nucleosome traps the ARM of Set1 at the interface, which adopts an α-helical conformation and docks to the nucleosomal acidic patch. By pushing against the Set1 catalytic domain sitting on top of histone H2A, the Set1 ARM helix might act as a pivot and inhibit COMPASS by affecting the spatial configuration of the Set1 catalytic domain relative to the rest of the COMPASS subunits. Upon conjugation to histone H2B, Ub stabilizes the C-terminal half of the Set1 ARM helix (Figure S7B) and packs against Swd1, which plays a key role in nucleating and organizing the COMPASS CM. These interactions conceivably enable Ub to override the inhibitory effect of the Set1 ARM helix by allosterically modulating the packing of the Set1 catalytic domain against Swd1, Bre2, and Swd3, thereby altering the dynamic property of its active site.

Notably, in our enzymatic assay, the COMPASS eCM is more active than the full-length COMPASS complex toward both NCP and uNCP substrates (Figure 1B versus Figure 1D), suggesting that other components of the large N-terminal half of COMPASS that are missing in the COMPASS eCM also contribute to the suppression of enzymatic activity (Jeon et al., 2018; Kim et al., 2013). Furthermore, without the ARM of the nSET domain, the COMPASS CM also has detectable response to H2Bub, which is also reflected in the human MLL complexes. Recent high-resolution structures of MLL1/MLL3 bound to an H2Bub nucleosome displayed a highly similar binding mode to the NCP disk face as yeast COMPASS (Xue et al., 2019). Interestingly, Ub is found in multiple different locations along the MLL/RBBP5 interface, suggesting that without the Set1/SETD1A/SETD1B-specific ARM element, the stimulatory effect of H2Bub is less specific and pronounced. It is plausible that H2Bub might facilitate the binding of the enzymatic assembly to nucleosomes by restricting the topological rearrangement of COMPASS that favors nucleosome binding

(Figures S7F–S7H). Future studies will be needed to elucidate the detailed mechanisms of COMPASS regulation by H2Bub.

STAR★METHODS

Detailed methods are provided in the online version of this paper and include the following:

LEAD CONTACT AND MATERIALS AVAILABILITY

Further information and requests for resources and reagents should be directed to and will be fulfilled by the Lead Contact, Ning Zheng (nzheng@uw.edu). Unique and stable reagents generated in this study are available upon request.

EXPERIMENTAL MODEL AND SUBJECT DETAILS

For DNA extraction, *E.coli* DH5α was used. For bacmid production, *E.coli* DH10Bac was used. For baculovirus production and amplification, Sf9 insect cells were used. For protein expression, both *E.coli* BL21(DE3) and HighFive insect cells were used.

METHOD DETAILS

Protein expression and purification—COMPASS subunits were PCR amplified from *K. lactis* genomic DNA and subcloned into modified pFastBac vectors for expression in insect cells. Recombinant viruses were produced as per manufacturer instructions, and subsequently amplified in Sf9 monolayer cells to generate high titer viruses for protein expression in HighFive monolayer cells. Purification of the COMPASS subomplexes and mutants were done as previously described (Hsu et al., 2018).

Nucleosome reconstitution—Individual histones and the H3K4M mutant were expressed individually in BL21 DE3, and harvested 18 hours post-induction. Histone octamers were reconstituted using the “one-pot” refolding method as previously described (Lee et al., 2015). The 601-147 bp DNA sequence was excised from a plasmid containing 20 repeats of the sequence (McGinty et al., 2016). The plasmid backbone was removed using PEG precipitation, and the 147 insert was further purified by anion exchange chromatography, followed by desalting into TE buffer. Small scale titrations were done to determine a 1:1 DNA:histone ratio, followed up by a large scale dialysis to form nucleosomes (Dyer et al., 2004). Nucleosomes (WT and H3K4M) were stored at 4°C and used within a week of formation.

H2Bub-nucleosome reconstitution—Individual *Xenopus* histones, including the H3K4M and H2B K120C mutants, were purchased from the Protein Expression and Purification facility at Colorado State University (https://www.histonesource.com) as lyophilized powders. Ub G76C was expressed in BL21 DE3, and purified using a combination of acid precipitation followed by cation exchange chromatography. Purified Ub G76C was then dialyzed into water, and lyophilized for future use.

Generation of H2Bub was done essentially as previously described (Chatterjee et al., 2010). In brief, DTNP (2.0 mg, 6.45 mmol) was dissolved in 500 μL of a 3:1 (v/v) acetic acid:water

mixture and added to H2B K120C (3 mg, 0.22 μmol). The reaction was allowed to proceed for 12 h at 25°C, prior to purification by C4 semi-preparative RP-HPLC with a 30%–70% B gradient. This yielded 2.1 mg (68.4%) of the pure H2B K120C-5-nitro-2-pyridinesulfenyl (pNpys) disulfide adduct. The identity of the disulfide adduct was verified by ESI-MS (expected: 13,622 Da, observed: 13,623 ± 3 Da). The product was then lyophilized for subsequent Ub ligation.

1 equivalent of the lyophilzed H2B-pNpys adduct (1.5 mg, 0.108 μmol) and 2.1 equivalents of Ub G76C (2.0 mg, 0.232 μmol) were dissolved in 625 μL of reaction buffer consisting of 1M HEPES, 6 M Gn-HCl, pH 6.9. Reaction was allowed for 1 h at 25°C with continuous shaking. The reaction products were purified by C4 semi-preparative HPLC with a 30%–70% B gradient to yield H2Bub (1.2 mg, 74%). The identity of the disulfide adduct was verified by ESI-MS (expected: 22,081 Da, observed: 22,083 ± 2 Da). The H2Bub product was then lyophilized and stored at −80°C for histone octamer reconstitution.

H2Bub-containing octamers were assembled using the salt dialysis method (Dyer et al., 2004) and purified over a Superdex 200 Increase 10/300 column (GE Healthcare) equilibrated in 10 mM HEPES pH 7.5, 2 M NaCl. Peak fractions were pooled and stored at −80°C for future use. H2Bub-nucleosomes were reconstituted as described for unmodified nucleosomes.

COMPASS-nucleosome complex reconstitution—Purified COMPASS eCM subcomplex were added to 4-fold excess to NCP/uNCP, and allowed to mix at room temperature for 30 minutes before injection on to a Superdex 200 Increase 10/300 column (GE Healthcare) equilibrated in 10 mM HEPES pH 7.5,100 mM NaCl, 1 mM DTT, 0.05 mM SAM (NEB). Peak fractions were collected, analyzed by SDS-PAGE, and pooled. The complex was concentrated to 5 mg/mL, flash frozen, and stored at −80°C for future use.

Preformed COMPASS eCM-nucleosome complexes were incubated with 0.1% (v/v) gluteraldehyde for 10 minutes at room temperature, and then quenched with the addition of 50 mM Tris pH 7.5. Crosslinked complexes were then injected on to a Superdex 200 Increase 10/300 (GE Healthcare) equilibrated in 20 mM Tris pH 7.5, 100 mM NaCl, 1 mM DTT, 0.05 mM SAM (NEB). Peak fractions were analyzed by negative stain electron microscopy, and the best fractions were pooled and concentrated to 0.6 mg/mL, and stored at −80°C for future grid preparation.

Grid preparation and cryo-EM data collection—For cryoEM grid preparation, the complex (eCM-uNCP or eCM-NCP) was diluted to 0.3 mg/mL. 3 μL of the diluted material was applied to the holey side of a glow discharged (PELCO easiGlow) QuantiAu 1.2/1.3, 300 mesh grid (Quantifoil Micro Tools GmbH), and allowed to incubate for 1 minute at 4°C and 100% relative humidity. The grid was subsequently blotted for 3 s, plunge frozen into liquid ethane using a Vitrobot Mark IV system (Thermo Fisher Scientific), and stored in liquid nitrogen for data collection.

For eCM-uNCP, data collection was carried out on a Titan Krios transmission electron microscope (Thermo Fisher Scientific) operated at 300 kV, equipped with a post-column

Gatan Quantum GIF energy filter and a Gatan K2 Summit direct detector. Movie stacks were recorded automatically using the Leginon software (Suloway et al., 2005) at a magnification of 130K, resulting a physical pixel size of 1.056 Å. The K2 camera was operated in super-resolution counting mode during data acquisition, and the slit width of energy filter was set to be 20 eV. A total dose of 74 $e^{-}/Å^2$ spanning a 9 s exposure time was fractionated into 45 frames. The whole dataset comprising 6,958 movie stacks was collected in two sessions with a defocus range set between 1 μm and 3 μm.

Settings of data collection for the eCM-NCP complex was similar to that used for eCM-uNCP. Either a 60-frame movie stack (3,855 movie stacks) or a 45-frame movie stack (10,336 movie stacks) was collected within a 9 s exposure, with a defocus range of 1~3 μm, and the total dose contained 74 $e^{-}/Å^2$. In total, 14,191 movie stacks were collected in five sessions.

Cryo-EM data processing of COMPASS eCM-uNCP—All data processing steps were implemented within the RELION-3.0 pipeline (Kimanius et al., 2016; Zivanov et al., 2018) unless mentioned explicitly. Both dose-weighted summed images and non-dose-weighted summed images with a pixel size of 1.056 Å were generated through aligning movie frames using MotionCor2 (Zheng et al., 2017), and binned by a factor of 2 in both dimensions by Fourier cropping. Images were then imported into cisTEM (Grant et al., 2018) for manual inspection. Images with ice of bad qualities or of unreasonable thickness were excluded. A subset of 6,036 high quality images was used for automatic particle picking in cisTEM, resulting in a set of 426,260 particles. The particle coordinates were exported in the Relion format for further processing. Parameters of the contrast transfer function (CTF) were estimated on the non-dose-weighted summed images by GCTF (Zhang, 2016). Particles were then extracted from the dose-weighted summed images.

A stack of 357,811 particles was created after data cleaning by 2 rounds of reference-free 2D classification. Global 3D classification without masking provided an initial model generated from RELION-3.0 was then performed to further classify the particles into 4 classes, in which the uNCP and one copy of the COMPASS eCM were better resolved, while the other copy of COMPASS eCM was less clear. To obtain a better class of eCM-uNCP complex, the set of 357,811 particles after 2D classification was subjected to a focused 3D classification procedure with a soft mask imposed, which enclosed both the uNCP and the better resolved copy of COMPASS eCM. Particles belonging to the best class from the last 6 iterations were combined, and duplicated particles were removed, giving rise to a particle set of 215,199 particles. This subset of particles went through focused 3D refinement with the same mask applied, resulting in a 3.6 Å density map. To further improve the quality of the reconstruction, particles used in the focused 3D refinement were imported for beam tilt parameters estimation in the CTF refinement job type (Zivanov et al., 2018) in RELION-3.0. The final density map was refined to a resolution of 3.5 Å by another round of focused refinement. The post-processing protocol in RELION-3.0 was used to correct for the modulation transfer function, sharpen the density map, and calculate the gold-standard Fourier shell correlation (FSC). According to the FSC 0.143 criterion (Rosenthal and Henderson, 2003), the reported resolution of the map is 3.5 Å. The map was sharpened by

applying a global B-factor of −123 $Å^2$ estimated during post-processing. Local resolution was determined by ResMap (Kucukelbir et al., 2014).

Cryo-EM data processing of COMPASS eCM-NCP—Image processing of COMPASS eCM-NCP was similar as that of eCM-uNCP. Movie frame alignment was carried out using MotionCor2 (Zheng et al., 2017), and binned by a factor of 2 in both dimensions by Fourier cropping. Both dose-weighted summed images and non-dose-weighted summed images with a pixel size of 1.056 Å were generated for later process. Summed images were imported into cisTEM (Grant et al., 2018) for manual inspection. A subset of 12,342 images with good ice quality and thickness were selected for later processing. 1,547,866 particles were automatically picked in cisTEM (Grant et al., 2018) on the good images, and coordinates were exported to RELION-3.0 for particle extraction. CTF parameters estimation for each individually picked particle were performed by GCTF (Zhang, 2016).

A pool of 1,547,866 particles were extracted from dose-weighted summed images and subjected to 2 rounds of reference-free 2D classification for particle clean up. A subset of 955,956 particles was obtained by selecting good 2D class averages. Initial model was created in RELION-3.0 and used for global 3D classification without masking. After merging and removing duplicated of particle assigned to the best class from the last 3 iterations, 221,787 particles were refined with a soft mask applied, which encompassed both the nucleosome core particle and a copy of the COMPASS eCM complex that showed a clearer density. A 3.76 Å density map was produced from the 3D refinement. To obtain a better density map, CTF refinement (Zivanov et al., 2018) was employed to estimate the beam tilt parameters, similar to that was done for the eCM-uNCP complex. In addition, Bayesian polishing (Zivanov et al., 2019) in RELION-3.0 was carried out to generate shiny particles. The set of 221,787 shiny particles were further processed by a second round of focused global 3D classification, with a finer angular search step (3.7°) and a τ value of 20. The final dataset comprised of 100,905 shiny particles and a 3.7 Å density map was generated after 3D auto-refine. The reconstructed map was post-processed in RELION-3.0. A global B-factor of −91 $Å^2$ estimated during post-processing was applied to sharpen the map. The final resolution was determined to be 3.7 Å based on the FSC 0.143 criterion (Rosenthal and Henderson, 2003). ResMap (Kucukelbir et al., 2014) was used for local resolution determination.

Model building and refinement—PDB crystal structures for the COMPASS CM (PDB: 6CHG), Ubiquitin (PDB: 1UBQ), NCP assembled with a 601 positioning sequence (PDB: 3MVD), and a homology model for *K.lactis* Spp1 generated from an HHPred alignment (Söding et al., 2005) and Modeler (Eswar et al., 2006) were rigid-body fit into the COMPASS eCM-uNCP density map using Chimera (Pettersen et al., 2004). The models were then manually trimmed, extended, and adjusted in Coot (Emsley and Cowtan, 2004). Models were then subject to several rounds of both local and global real-space refinement in Coot and Phenix (Adams et al., 2010). Statistics of the final refinement are reported in Table S1. Model building and refinement were done similarly for the COMPASS eCM-NCP complex.

Methyltransferase assays—1 μM of enzyme and 0.5 μM of nucleosome/H2Bub-nucleosome substrates were incubated in buffer containing 20 mM HEPES pH 7.5,100 mM NaCl, and 0.2 mM SAM (NEB) for 15 minutes at 30°C. Reactions were quenched with the addition of SDS-PAGE loading buffer, resolved on a 15% gel, and transferred to PVDF membranes. Membranes were blocked at room temperature in 5% milk in TBS-T, and then probed with antibodies against H3 (Abcam ab1791), H3K4me1 (CST D1A9), H3K4me2 (Abcam ab7766), and H3K4me3 (Abcam ab8580) overnight at 4°C. Blots were washed the next morning with TBS-T and then probed with secondary antibody at room temperature for 1 hour. Blots were subsequently washed with TBS-T to remove excess secondary. The blots were then incubated with ECL reagent, and exposed on an imager for analysis.

Nucleosome binding assays—50 nM H3K4M-nucleosome/H2Bub-nucleosome were incubated with increasing concentrations of COMPASS complexes (0.1 μM, 0.25 μM, 0.5 μM, 1.0 μM, 2.5 μM, 5.0 μM) in a buffer containing 20 μM HEPES pH 7.5, 50 μM NaCl, 0.05 μM SAM (NEB) for 30 minutes at room temperature. Glycerol was then added to a final concentration of 10%, and then loaded into a pre-chilled, pre-run 5% (29:1) 0.2X TBE native acrylamide gel. Gels were run at 120V for 90 minutes, and then stained with SybrGold, and exposed on an imager for analysis.

QUANTIFICATION AND STATISTICAL ANALYSIS

Protein quantification was done using Bio-Rad Protein Assay Dye, and comparing the readings against a standard curve generated using BSA. Nucleosome concentrations were determined using an A260 extinction coefficient of 2,784,500 $M^{-1}cm^{-1}$ on a Nanodrop spectrophotometer (Thermo Fisher).

DATA AND CODE AVAILABILITY

The accession number for the cryo-EM map of the COMPASS eCM-uNCP, and eCM-NCP complex are EMD: 20767 and EMD: 20765, respectively. The coordinates for the COMPASS eCM-uNCP, and eCM-NCP is deposited under the accession numbers PDB: 6UH5 and PDB: 6UGM, respectively.

Supplementary Material

Refer to Web version on PubMed Central for supplementary material.

ACKNOWLEDGMENTS

We would like to thank Joel Quispe (UW Biochemistry EM facility) for assistance and training in EM sample preparation, microscope operation, and data collection. We would also like to thank the Colorado State University Protein Expression and Purification facility for individual histone proteins. The plasmids for expression of *Xenopus* histones were a kind gift from Dr. Karolin Luger. This work was supported by the Howard Hughes Medical Institute (N.Z.) and the NIH (2R01GM110430-06; C.C.).

REFERENCES

Adams PD, Afonine PV, Bunkóczi G, Chen VB, Davis IW, Echols N, Headd JJ, Hung LW, Kapral GJ, Grosse-Kunstleve RW, et al. (2010). PHENIX: a comprehensive Python-based system for

macromolecular structure solution. Acta Crystallogr. D Biol. Crystallogr 66, 213–221. [PubMed: 20124702]

Anderson CJ, Baird MR, Hsu A, Barbour EH, Koyama Y, Borgnia MJ, and McGinty RK (2019). Structural basis for recognition of ubiquitylated nucleosome by Dot1L methyltransferase. Cell Rep. 26, 1681–1690.e5. [PubMed: 30759380]

Ardehali MB, Mei A, Zobeck KL, Caron M, Lis JT, and Kusch T (2011). Drosophila Set1 is the major histone H3 lysine 4 trimethyltransferase with role in transcription. EMBO J. 30, 2817–2828. [PubMed: 21694722]

Cao F, Chen Y, Cierpicki T, Liu Y, Basrur V, Lei M, and Dou Y (2010). An Ash2L/RbBP5 heterodimer stimulates the MLL1 methyltransferase activity through coordinated substrate interactions with the MLL1 SET domain. PLoS ONE 5, e14102. [PubMed: 21124902]

Chatterjee C, McGinty RK, Fierz B, and Muir TW (2010). Disulfide-directed histone ubiquitylation reveals plasticity in hDot1L activation. Nat. Chem. Biol 6, 267–269. [PubMed: 20208522]

Chen Y, Wan B, Wang KC, Cao F, Yang Y, Protacio A, Dou Y, Chang HY, and Lei M (2011). Crystal structure of the N-terminal region of human Ash2L shows a winged-helix motif involved in DNA binding. EMBO Rep. 12, 797–803. [PubMed: 21660059]

Denissov S, Hofemeister H, Marks H, Kranz A, Ciotta G, Singh S, Anastassiadis K, Stunnenberg HG, and Stewart AF (2014). Mll2 is required for H3K4 trimethylation on bivalent promoters in embryonic stem cells, whereas Mll1 is redundant. Development 141, 526–537. [PubMed: 24423662]

Dou Y, Milne TA, Ruthenburg AJ, Lee S, Lee JW, Verdine GL, Allis CD, and Roeder RG (2006). Regulation of MLL1 H3K4 methyltransferase activity by its core components. Nat. Struct. Mol. Biol 13, 713–719. [PubMed: 16878130]

Dyer PN, Edayathumangalam RS, White CL, Bao Y, Chakravarthy S, Muthurajan UM, and Luger K (2004). Reconstitution of nucleosome core particles from recombinant histones and DNA. Methods Enzymol. 375,23–44. [PubMed: 14870657]

Emsley P, and Cowtan K (2004). Coot: model-building tools for molecular graphics. Acta Crystallogr. D Biol. Crystallogr 60, 2126–2132. [PubMed: 15572765]

Eswar N, Webb B, Marti-Renom MA, Madhusudhan MS, Eramian D, Shen M, Pieper U, and Sali A (2006). Comparative protein structure modeling using Modeller. Curr. Protoc. Bioinformatics Chapter 5, Unit 5.6.

Grant T, Rohou A, and Grigorieff N (2018). *cis*TEM, user-friendly software for single-particle image processing. eLife 7, e35383. [PubMed: 29513216]

Halbach A, Zhang H, Wengi A, Jablonska Z, Gruber IML, Halbeisen RE, Dehé PM, Kemmeren P, Holstege F, Géli V, et al. (2009). Cotranslational assembly of the yeast SET1C histone methyltransferase complex. EMBO J. 28, 2959–2970. [PubMed: 19713935]

Herz HM, Mohan M, Garruss AS, Liang K, Takahashi YH, Mickey K, Voets O, Verrijzer CP, and Shilatifard A (2012). Enhancer-associated H3K4 monomethylation by Trithorax-related, the Drosophila homolog of mammalian Mll3/Mll4. Genes Dev. 26, 2604–2620. [PubMed: 23166019]

Holt MT, David Y, Pollock S, Tang Z, Jeon J, Kim J, Roeder RG, and Muir TW (2015). Identification of a functional hotspot on ubiquitin required for stimulation of methyltransferase activity on chromatin. Proc. Natl. Acad. Sci. USA 112, 10365–10370. [PubMed: 26240340]

Hsu PL, Li H, Lau HT, Leonen C, Dhall A, Ong SE, Chatterjee C, and Zheng N (2018). Crystal structure of the COMPASS H3K4 methyltransferase catalytic module. Cell 174, 1106–1116.e9. [PubMed: 30100181]

Hu D, Gao X, Morgan MA, Herz HM, Smith ER, and Shilatifard A (2013). The MLL3/MLL4 branches of the COMPASS family function as major histone H3K4 monomethylases at enhancers. Mol. Cell. Biol 33, 4745–4754. [PubMed: 24081332]

Jang S, Kang C, Yang HS, Jung T, Hebert H, Chung KY, Kim SJ, Hohng S, and Song JJ (2019). Structural basis of recognition and destabilization of the histone H2B ubiquitinated nucleosome by the DOT1L histone H3 Lys79 methyltransferase. Genes Dev. 33, 620–625. [PubMed: 30923167]

Jeon J, McGinty RK, Muir TW, Kim JA, and Kim J (2018). Crosstalk among Set1 complex subunits involved in H2B ubiquitylation-dependent H3K4 methylation. Nucleic Acids Res. 46, 11129–11143. [PubMed: 30325428]

Kim J, Kim JA, McGinty RK, Nguyen UTT, Muir TW, Allis CD, and Roeder RG (2013). The n-SET domain of Set1 regulates H2B ubiquitylation-dependent H3K4 methylation. Mol. Cell 49, 1121–1133. [PubMed: 23453808]

Kimanius D, Forsberg BO, Scheres SH, and Lindahl E (2016). Accelerated cryo-EM structure determination with parallelisation using GPUs in RELION-2. eLife 5, e18722. [PubMed: 27845625]

Krogan NJ, Dover J, Khorrami S, Greenblatt JF, Schneider J, Johnston M, and Shilatifard A (2002). COMPASS, a histone H3 (Lysine 4) methyltransferase required for telomeric silencing of gene expression. J. Biol. Chem 277, 10753–10755. [PubMed: 11805083]

Kucukelbir A, Sigworth FJ, and Tagare HD (2014). Quantifying the local resolution of cryo-EM density maps. Nat. Methods 11, 63–65. [PubMed: 24213166]

Lee JE, Wang C, Xu S, Cho YW, Wang L, Feng X, Baldridge A, Sartorelli V, Zhuang L, Peng W, and Ge K (2013). H3K4 mono- and di-methyltransferase MLL4 is required for enhancer activation during cell differentiation. eLife 2, e01503. [PubMed: 24368734]

Lee YT, Gibbons G, Lee SY, Nikolovska-Coleska Z, and Dou Y (2015). One-pot refolding of core histones from bacterial inclusion bodies allows rapid reconstitution of histone octamer. Protein Expr. Purif 110, 89–94. [PubMed: 25687285]

Li Y, Han J, Zhang Y, Cao F, Liu Z, Li S, Wu J, Hu C, Wang Y, Shuai J, et al. (2016). Structural basis for activity regulation of MLL family methyltransferases. Nature 530, 447–452. [PubMed: 26886794]

McGinty RK, and Tan S (2016). Recognition of the nucleosome by chromatin factors and enzymes. Curr. Opin. Struct. Biol 37, 54–61. [PubMed: 26764865]

McGinty RK, Kim J, Chatterjee C, Roeder RG, and Muir TW (2008). Chemically ubiquitylated histone H2B stimulates hDot1L-mediated intranucleosomal methylation. Nature 453, 812–816. [PubMed: 18449190]

McGinty RK, Henrici RC, and Tan S (2014). Crystal structure of the PRC1 ubiquitylation module bound to the nucleosome. Nature 514, 591–596. [PubMed: 25355358]

McGinty RK, Makde RD, and Tan S (2016). Preparation, crystallization and structure determination of chromatin enzyme/nucleosome complexes. Methods Enzymol. 573, 43–65. [PubMed: 27372748]

Mersman DP, Du HN, Fingerman IM, South PF, and Briggs SD (2012). Charge-based interaction conserved within histone H3 lysine 4 (H3K4) methyltransferase complexes is needed for protein stability, histone methylation, and gene expression. J. Biol. Chem 287, 2652–2665. [PubMed: 22147691]

Miller T, Krogan NJ, Dover J, Erdjument-Bromage H, Tempst P, Johnston M, Greenblatt JF, and Shilatifard A (2001). COMPASS: a complex of proteins associated with a trithorax-related SET domain protein. Proc. Natl. Acad. Sci. USA 98, 12902–12907. [PubMed: 11687631]

Morgan MT, Haj-Yahya M, Ringel AE, Bandi P, Brik A, and Wolberger C (2016). Structural basis for histone H2B deubiquitination by the SAGA DUB module. Science 351, 725–728. [PubMed: 26912860]

Nagy PL, Griesenbeck J, Kornberg RD, and Cleary ML (2002). A trithorax-group complex purified from Saccharomyces cerevisiae is required for methylation of histone H3. Proc. Natl. Acad. Sci. USA 99, 90–94. [PubMed: 11752412]

Nakanishi S, Sanderson BW, Delventhal KM, Bradford WD, Staehling-Hampton K, and Shilatifard A (2008).A comprehensive library of histone mutants identifies nucleosomal residues required for H3K4 methylation. Nat. Struct. Mol. Biol 15, 881–888. [PubMed: 18622391]

Patel A, Dharmarajan V, Vought VE, and Cosgrove MS (2009). On the mechanism of multiple lysine methylation by the human mixed lineage leukemia protein-1 (MLL1) core complex. J. Biol. Chem 284, 24242–24256. [PubMed: 19556245]

Pettersen EF, Goddard TD, Huang CC, Couch GS, Greenblatt DM, Meng EC, and Ferrin TE (2004). UCSF Chimera-a visualization system for exploratory research and analysis. J. Comput. Chem 25, 1605–1612. [PubMed: 15264254]

Qu Q, Takahashi YH, Yang Y, Hu H, Zhang Y, Brunzelle JS, Couture JF, Shilatifard A, and Skiniotis G (2018). Structure and conformational dynamics of a COMPASS histone H3K4 methyltransferase complex. Cell 174, 1117–1126.e12. [PubMed: 30100186]

Roguev A, Schaft D, Shevchenko A, Pijnappel WWMP, Wilm M, Aasland R, and Stewart AF (2001). The Saccharomyces cerevisiae Set1 complex includes an Ash2 homologue and methylates histone 3 lysine 4. EMBO J. 20, 7137–7148. [PubMed: 11742990]

Rosenthal PB, and Henderson R (2003). Optimal determination of particle orientation, absolute hand, and contrast loss in single-particle electron cryomicroscopy. J. Mol. Biol 333, 721–745. [PubMed: 14568533]

Shilatifard A (2012). The COMPASS family of histone H3K4 methylases: mechanisms of regulation in development and disease pathogenesis. Annu. Rev. Biochem 81, 65–95. [PubMed: 22663077]

Shinsky SA, Hu M, Vought VE, Ng SB, Bamshad MJ, Shendure J, and Cosgrove MS (2014). A non-active-site SET domain surface crucial for the interaction of MLL1 and the RbBP5/Ash2L heterodimer within MLL family core complexes. J. Mol. Biol 426, 2283–2299. [PubMed: 24680668]

Shinsky SA, Monteith KE, Viggiano S, and Cosgrove MS (2015). Biochemical reconstitution and phylogenetic comparison of human SET1 family core complexes involved in histone methylation. J. Biol. Chem 290, 6361–6375. [PubMed: 25561738]

Söding J, Biegert A, and Lupas AN (2005). The HHpred interactive server for protein homology detection and structure prediction. Nucleic Acids Res. 33, W244–8. [PubMed: 15980461]

Southall SM, Wong PS, Odho Z, Roe SM, and Wilson JR (2009). Structural basis for the requirement of additional factors for MLL1 SET domain activity and recognition of epigenetic marks. Mol. Cell 33, 181–191. [PubMed: 19187761]

Sprague ER, Redd MJ, Johnson AD, and Wolberger C (2000). Structure of the C-terminal domain of Tup1, a corepressor of transcription in yeast. EMBO J. 19, 3016–3027. [PubMed: 10856245]

Suloway C, Pulokas J, Fellmann D, Cheng A, Guerra F, Quispe J, Stagg S, Potter CS, and Carragher B (2005). Automated molecular microscopy: the new Leginon system. J. Struct. Biol 151, 41–60. [PubMed: 15890530]

Sun ZW, and Allis CD (2002). Ubiquitination of histone H2B regulates H3 methylation and gene silencing in yeast. Nature 418, 104–108. [PubMed: 12077605]

Trésaugues L, Dehé PM, Guérois R, Rodriguez-Gil A, Varlet I, Salah P, Pamblanco M, Luciano P, Quevillon-Cheruel S, Sollier J, et al. (2006). Structural characterization of Set1 RNA recognition motifs and their role in histone H3 lysine 4 methylation. J. Mol. Biol 359, 1170–1181. [PubMed: 16787775]

Valencia-Sánchez MI, De loannes P, Wang M, Vasilyev N, Chen R, Nudler E, Armache JP, and Armache KJ (2019). Structural basis of Dot1L stimulation by histone H2B lysine 120 ubiquitination. Mol. Cell 74, 1010–1019.e6. [PubMed: 30981630]

Wang P, Lin C, Smith ER, Guo H, Sanderson BW, Wu M, Gogol M, Alexander T, Seidel C, Wiedemann LM, et al. (2009). Global analysis of H3K4 methylation defines MLL family member targets and points to a role for MLL1-mediated H3K4 methylation in the regulation of transcriptional initiation by RNA polymerase II. Mol. Cell. Biol 29, 6074–6085. [PubMed: 19703992]

Wang L, Cao C, Wang F, Zhao J, and Li W (2017). H2B ubiquitination: Conserved molecular mechanism, diverse physiologic functions of the E3 ligase during meiosis. Nucleus 8, 461–468. [PubMed: 28628358]

Winget JM, and Mayor T (2010). The diversity of ubiquitin recognition: hot spots and varied specificity. Mol. Cell 38, 627–635. [PubMed: 20541996]

Worden EJ, and Wolberger C (2019). Activation and regulation of H2B-Ubiquitin-dependent histone methyltransferases. Curr. Opin. Struct. Biol 59,98–106. [PubMed: 31229920]

Worden EJ, Hoffmann NA, Hicks CW, and Wolberger C (2019). Mechanism of cross-talk between H2B ubiquitination and H3 methylation by Dot1L. Cell 176, 1490–1501.e12. [PubMed: 30765112]

Wu M, Wang PF, Lee JS, Martin-Brown S, Florens L, Washburn M, and Shilatifard A (2008). Molecular regulation of H3K4 trimethylation by Wdr82, a component of human Set1/COMPASS. Mol. Cell. Biol 28, 7337–7344. [PubMed: 18838538]

Xue H, Yao T, Cao M, Zhu G, Li Y, Yuan G, Chen Y, Lei M, and Huang J (2019). Structural basis of nucleosome recognition and modification by MLL methyltransferases. Nature 573, 445–449. [PubMed: 31485071]

Zhang K (2016). Gctf: Real-time CTF determination and correction. J. Struct. Biol 193, 1–12. [PubMed: 26592709]

Zhang Y, Mittal A, Reid J, Reich S, Gamblin SJ, and Wilson JR (2015). Evolving catalytic properties of the MLL family SET domain. Structure 23, 1921–1933. [PubMed: 26320581]

Zheng SQ, Palovcak E, Armache JP, Verba KA, Cheng Y, and Agard DA (2017). MotionCor2: anisotropic correction of beam-induced motion for improved cryo-electron microscopy. Nat. Methods 14, 331–332. [PubMed: 28250466]

Zivanov J, Nakane T, Forsberg BO, Kimanius D, Hagen WJ, Lindahl E, and Scheres SH (2018). New tools for automated high-resolution cryo-EM structure determination in RELION-3. eLife 7, e42166. [PubMed: 30412051]

Zivanov J, Nakane T, and Scheres SHW (2019). A Bayesian approach to beam-induced motion correction in cryo-EM single-particle analysis. IUCrJ 6, 5–17.

Highlights

- Cryo-EM structures of COMPASS bound to a H2B-ubiquitinated and unmodified nucleosome
- COMPASS captures nucleosomes by extensive interfacing with both histones and DNA
- The Set1 ARM helix autoinhibits COMPASS upon nucleosome binding
- H2Bub allosterically activates COMPASS by anchoring to the Set1 ARM helix

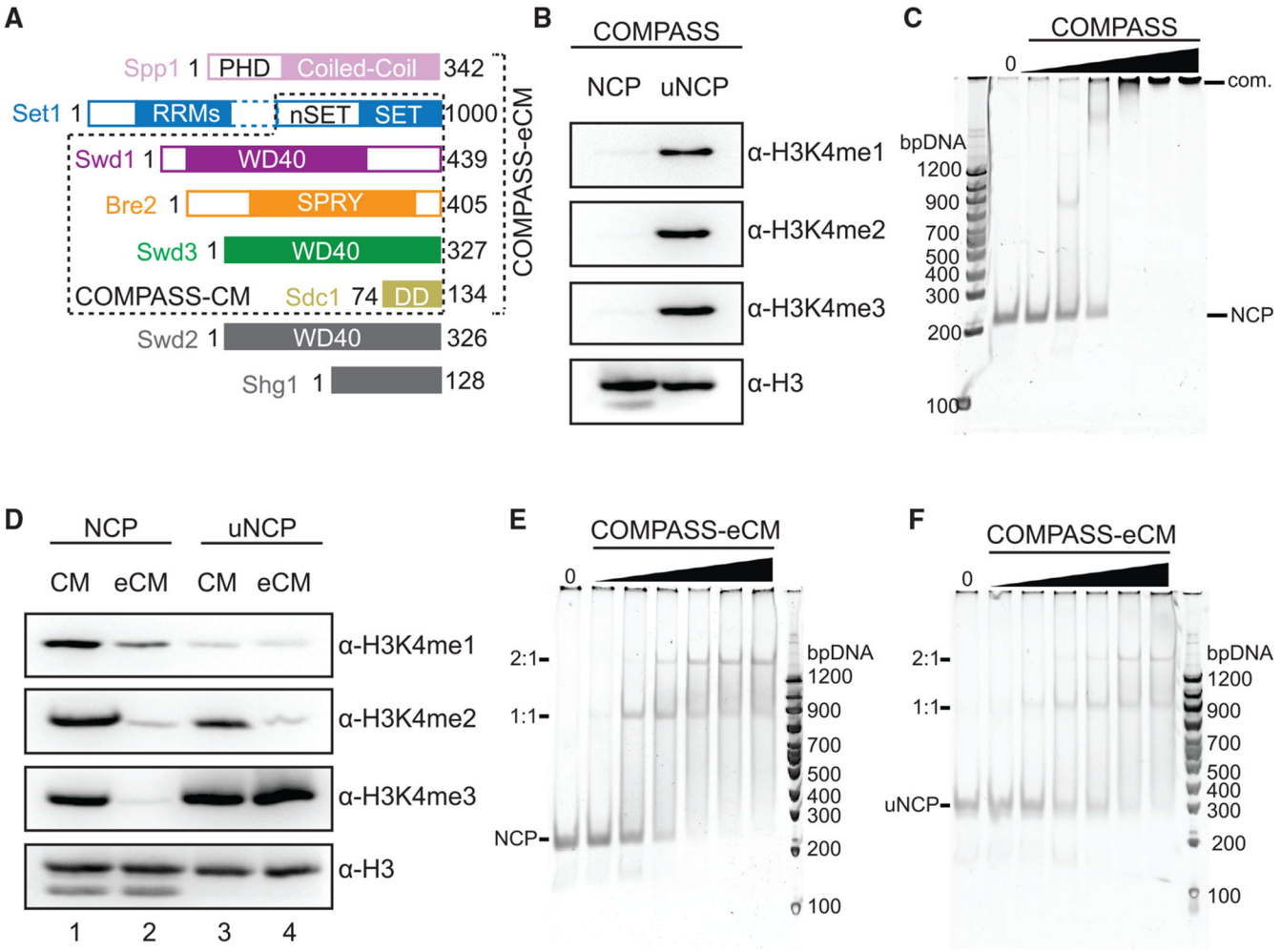

Figure 1. Biochemical Analyses of COMPASS Nucleosomal Binding and Activity

(A) Domain organization and construct design of COMPASS subunits utilized in biochemical analysis and structure determination. Set1 is not drawn to scale. The dotted box between the nSET and RRM domains indicates a long linker region. The CM boxed in dashed lines contains the Set1 SET domain and the four WRAD subunits. The eCM extends the CM by including the nSET domain and its binding partner, Spp1.

(B) H3K4 methyltransferase activity of purified full-length COMPASS on NCP and uNCP substrates. COMPASS exhibits little to no activity on unmodified nucleosomes while displaying robust methylation on ubiquitinated nucleosomes like its *S. cerevisiae* ortholog.

(C) Native Tris-borate-EDTA (TBE) gel shift assay of unmodified nucleosomes with increasing concentrations of COMPASS, stained by SybrGold.

(D) H3K4 methyltransferase activity of both the COMPASS catalytic module (CM) and extended CM (eCM) on NCP and uNCP substrates. eCM activity is largely suppressed on unmodified nucleosomes and greatly stimulated by H2Bub nucleosomes.

(E) Native TBE gel shift assay of unmodified nucleosomes with increasing concentrations of COMPASS-eCM, stained by SybrGold.

(F) Native TBE gel shift assay of H2Bub nucleosomes with increasing concentrations of COMPASS-eCM, stained by SybrGold.

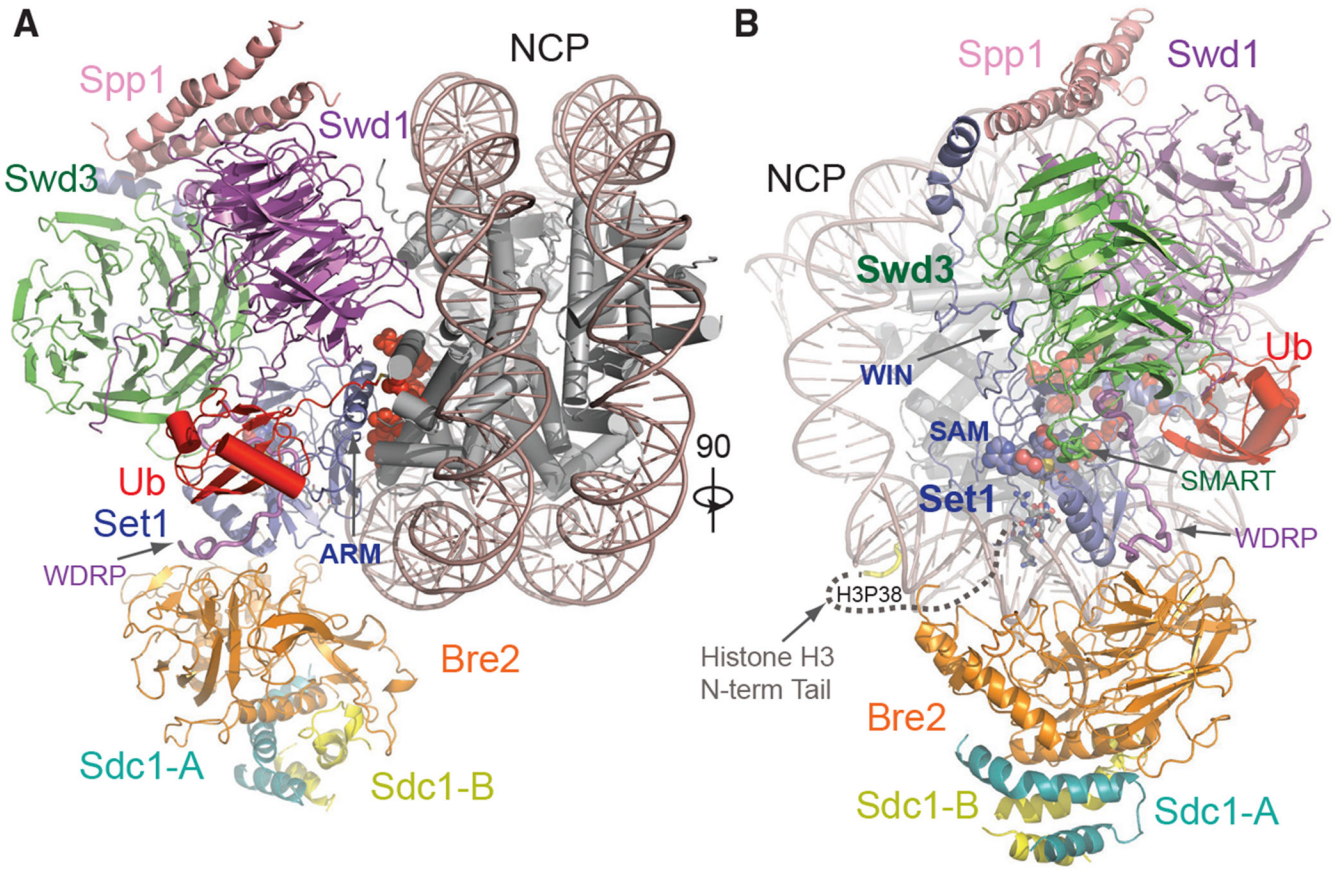

Figure 2. Overall Structure of the COMPASS eCM-uNCP Complex

(A) Model of COMPASS-eCM bound to the H2Bub modified nucleosome. Set1 (blue), Swd1 (magenta), Swd3 (green), Bre2 (orange), Sdc1-A and B (turquoise and yellow), Spp1 (pink), and Ub (red) are shown in cartoon form. Nucleosomal DNA (dark salmon) is shown in cartoon form. The histone octamer is shown in cylinders. The SAM cofactor is shown in space-filling form. Residues forming the H2A-H2B acidic patch are shown in red spheres. The positions of the Swd1 WDRP and Set1 ARM helix are indicated by arrows.

(B) View of (A) rotated 90° and colored in the same scheme. The positions of the Set1 WIN motif (tube form), Swd3 SMART motif (tube), and Swd1 WDRP (tube) are indicated by arrows. A dashed line indicates the flexible histone H3 N-terminal tail spanning residue 9–38, which connects the first stretch of H3 seen in the NCP body (yellow tube) and the H3 (A1-R8) peptide (sticks) found in the Set1 SET domain.

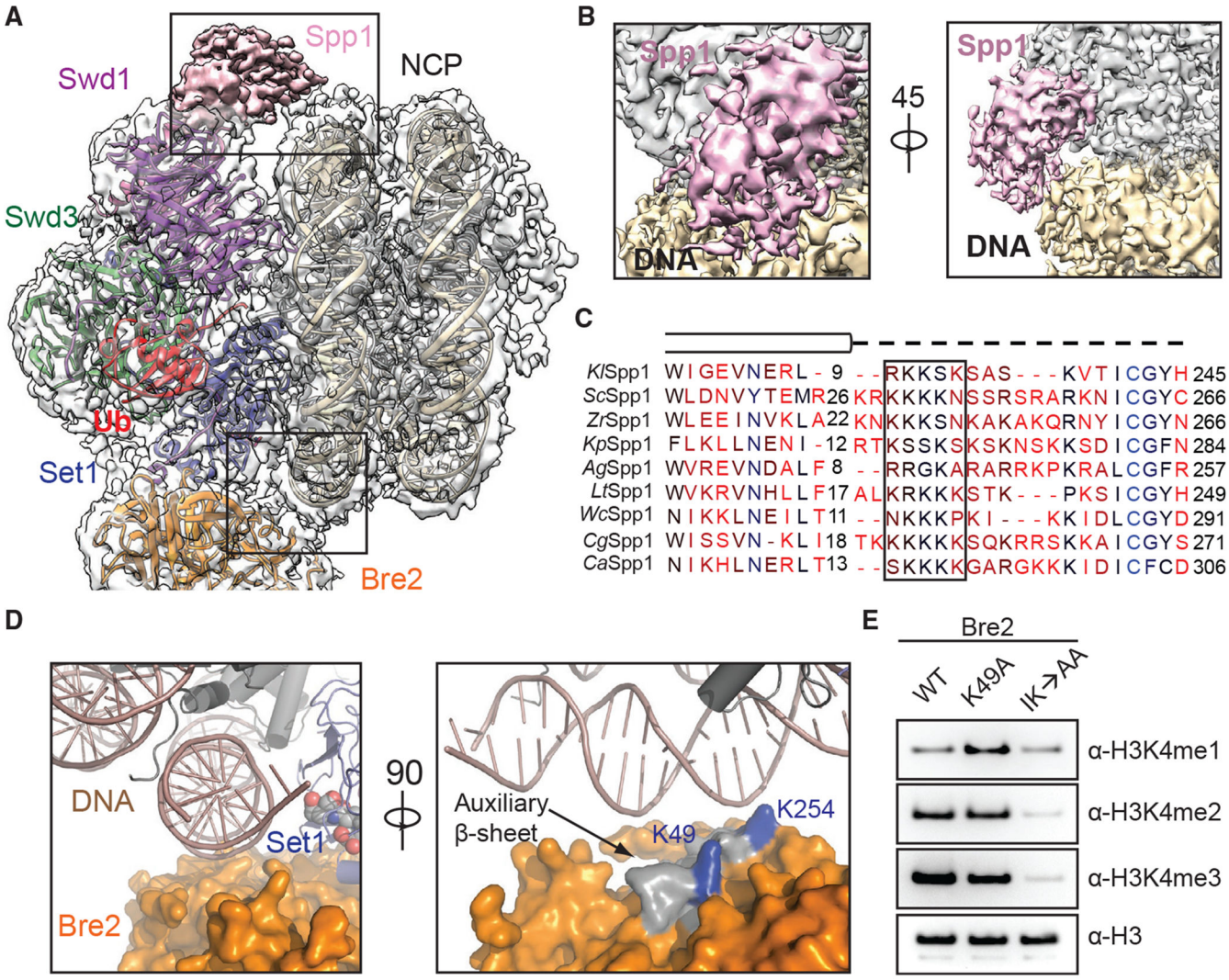

Figure 3. DNA Binding Stabilizes COMPASS on Nucleosomes

(A) Zoom-out view of the complex structure superimposed on the cryo-EM map. Major DNA-binding sites are boxed. Swd1 is shown in magenta, Swd3 in green, Set1 in blue, Bre2 in orange, Spp1 in pink, Ub in red, histones in dark gray, and nucleosomal DNA in wheat.

(B) Close-up views of the Spp1 DNA-binding domain density (pink) on nucleosomal DNA (wheat) in two different orientations.

(C) Structure-based sequence alignment of yeast Spp1 orthologs from *K. lactis* (*Kl*), *S. cerevisiae* (*Sc*), *Z. rouxii* (*Zr*), *K. pastoris* (*Kp*), *A. gossypii* (*Ag*), *L. thermotolerans* (*Lt*), *W. ciferri* (*Wc*), *C. glabrata* (*Cg*), and *C. albicans* (*Ca*). Cylinders denote α helices, while the dashed line indicates an unmodeled region, predicted to lack secondary structure. A basic region with potential DNA-binding function is boxed.

(D) Left: close-up view of Bre2 (orange in surface representation) looking down the nucleosomal DNA entry/exit point (cartoon representation, dark salmon). Right: 90° rotation of the left panel, highlighting the position of auxiliary β sheet (gray) on Bre2 relative to DNA. Two highly conserved lysine residues on the surface of this structural element are colored in blue.

(E) H3K4 methyltransferase activity of the COMPASS CM assembled with Bre2 mutants against nucleosomal substrates. The IK→AA double mutant of two conserved surface residues, Ile251 and Lys254, drastically reduces activity of the CM against H3K4.

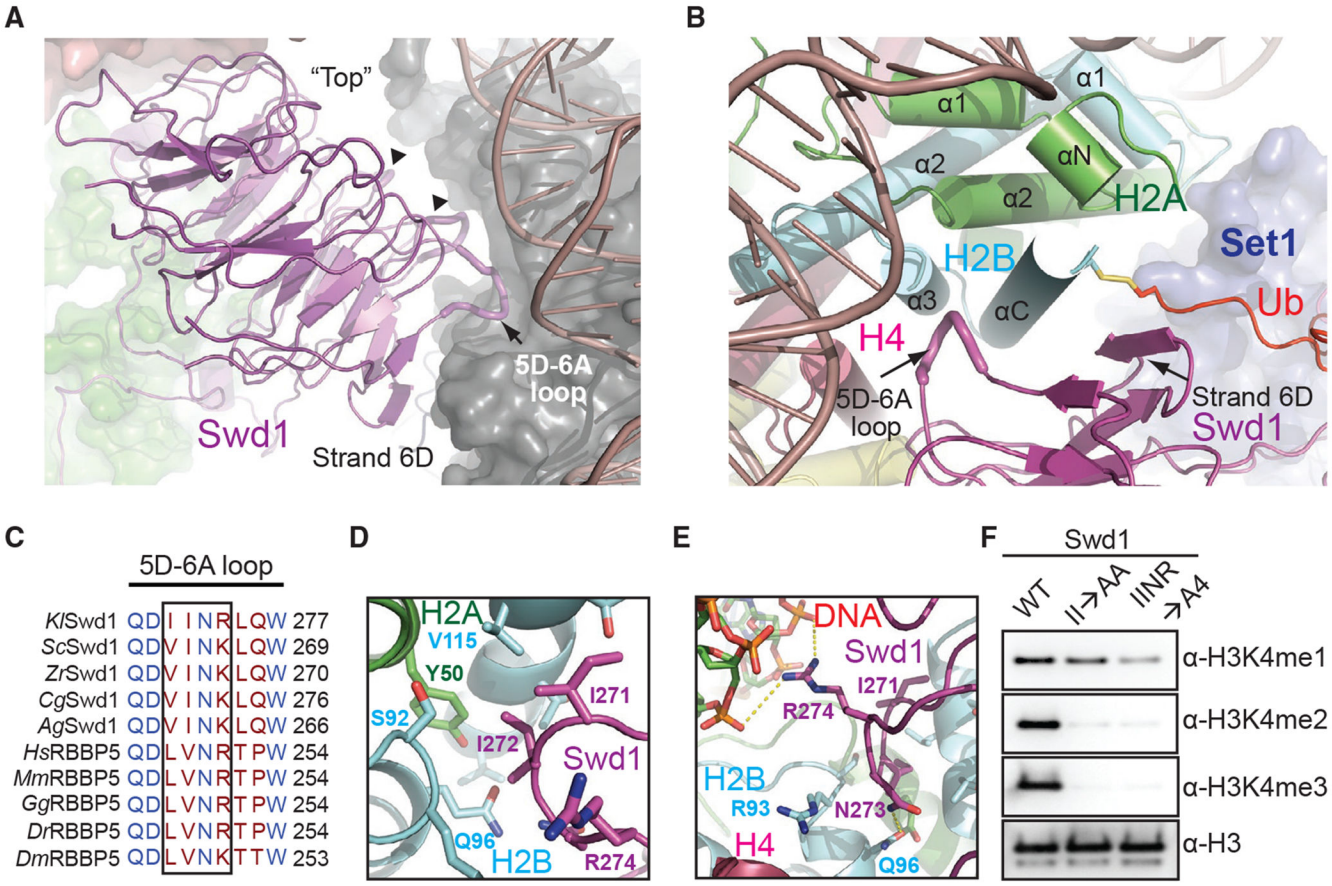

Figure 4. Swd1 Is a Histone-Binding Protein

(A) Side view of Swd1 (magenta, cartoon) positioned over the histone surface (dark gray, surface). The "top" face of the WD40 is pointed toward the nucleosome, while the "bottom" is facing COMPASS, interacting with Swd3 (green, surface). The top surface loops interacting with the histone surface are shown in tube representation. The 5D-6A loop (tube form) and strand D from blade 6 are labeled. The two loops interacting with H3 and H4 are indicated by triangles.

(B) Top-down view, looking down the C-terminal H2B helix (cyan). Swd1 (magenta) wraps around this helix using the 5D-6A loop (tube form) and strand 6D. Set1 is shown in blue surface representation. H2A and H4 are shown in green and deep red, respectively, in cartoon form. The C-terminal tail of Ub (red) is fused to H2B via a disulfide linkage.

(C) Local structure-based sequence alignment of the 5D-6A loop across *K. lactis* (*Kl*), *S. cerevisiae* (Sc), *Z. rouxii* (*Zr*), *C. glabrata* (*Cg*), *A. gossypii* (*Ag*), *H. sapiens* (*Hs*), *M. muscuius* (*Mm*), *G. gallus* (*Gg*), *D. rerio* (*Dr*), and *D. meianogaster* (*Dm*) orthologs. Straight line denotes an element with no secondary structure. The four-residue segment that inserts itself into the H2A-H2B three-helix cleft is boxed.

(D) Close-up view centered on the two conserved hydrophobic residues in the 5D-6A loop (magenta) at the three-helix juncture (H2B in cyan, H2A in green).

(E) Close-up view centered on the two polar residues in the 5D-6A loop (magenta). Asn273 forms a hydrogen bond with H2B Gln96 (cyan), while Arg274 interacts with the phosphate

backbone of nucleosomal DNA (red, sticks). Polar and salt bridge interactions are shown as dotted yellow lines.

(F) H3K4 methyltransferase activity of the COMPASS CM assembled with Swd1 5D-6A loop mutants against nucleosomal substrates. A double mutant of two hydrophobic residues (II→AA) reduces methyltransferase activity to monomethylation. A quadruple mutant (IINR→A4) nearly renders the CM inactive.

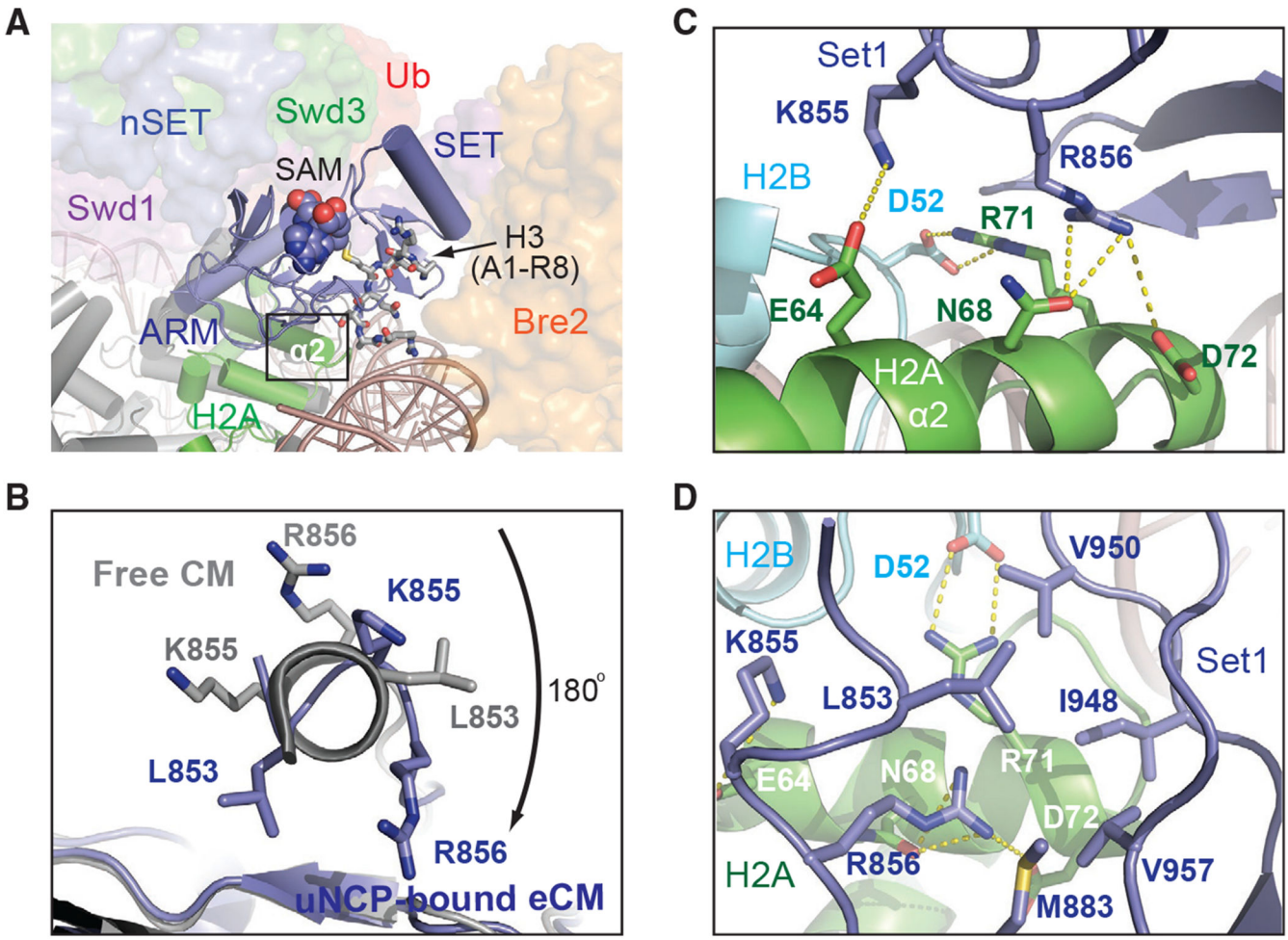

Figure 5. The SET N Terminus Unravels to Bind H2A

(A) Zoom-out view of Set1-SET (blue, cartoon) being positioned over histone H2A (green) and sandwiched by Bre2 (orange, surface) and Swd1 (magenta, surface). Swd3 (green) and the nSET domain (blue) are also shown in surface representation. The cofactor SAM and the H3 N terminus are shown in space-filling and stick form, respectively. Boxed is the region of interaction between Set1 and H2A.

(B) View looking down the N-terminal helix of the Set1 SET domain. The SET domain found in the NCP-bound structure is shown in blue, while the free form of the SET domain is shown in gray. Residues involved in interacting with H2A upon helical unraveling are shown in sticks.

(C) Close-up view of the rearranged Set1 N terminus (blue) presenting both Lys855 and Arg856 into a polar tip found on H2A α2 helix (green). Hydrogen bonds and salt bridges are shown as dashed yellow lines.

(D) Close-up view of the Set1 hydrophobic claw (blue) interaction with H2A (green). H2B is shown in cyan. H3 and H4 are omitted for clarity. Set1, H2A, and H2B amino acids are labeled in blue, white, and cyan, respectively.

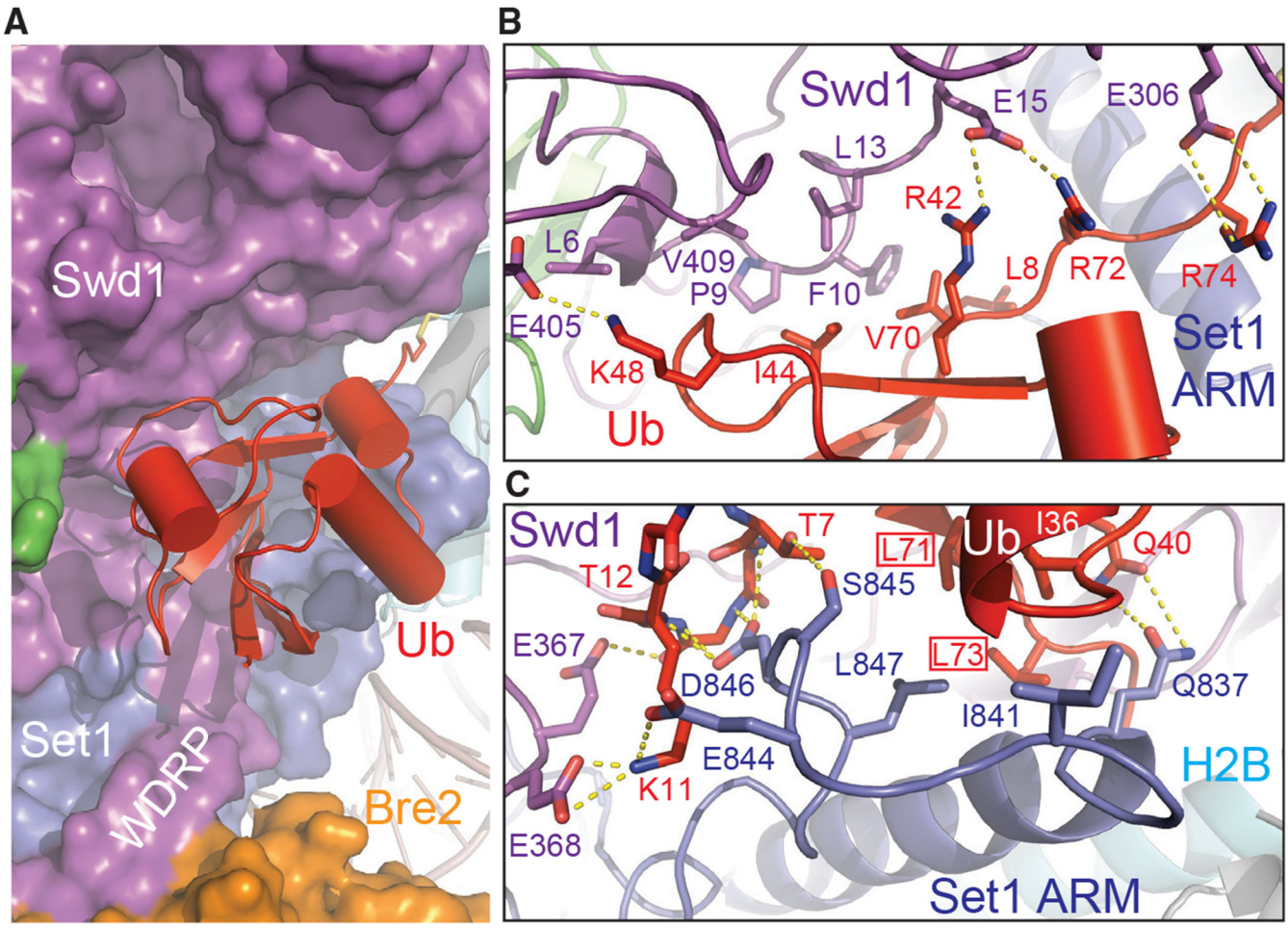

Figure 6. H2B~Ub Packs against Swd1 and Set1

(A) Zoom-out view of H2B~Ub (red, cartoon) against COMPASS. Swd1 (magenta), Set1 (blue), and Bre2 (orange) are shown in surface form. The disulfide linkage between H2B (cyan, cylinder) and Ub is shown in stick form. The critical WDRP necessary for Set1 activity is labeled.

(B) Close-up view of the interface between the Ub Ile44 hydrophobic patch and Swd1. Ub packs extensively against a series of conserved residues on Swd1 spread across its N terminus, WD40, and C-terminal tail. Key side chains are shown in sticks and labeled. Hydrogen bonds and salt bridges are shown as dashed yellow lines.

(C) Close-up view of the interface between the Set1 SET N terminus (blue) and Ub Ile36 underside site (red). The N terminus of the SET domain makes several backbone interactions with Ub between Thr7 and Thr12 (shown in sticks, side chains omitted for clarity). A series of Set1 hydrophobic residues pack against the base of the Ub helix. The Ub Leu71/Leu73 pair identified in Holt et al. (2015) critical for H2Bub-H3K4me crosstalk is boxed. Hydrogen bonds and salt bridges are shown as dashed yellow lines.

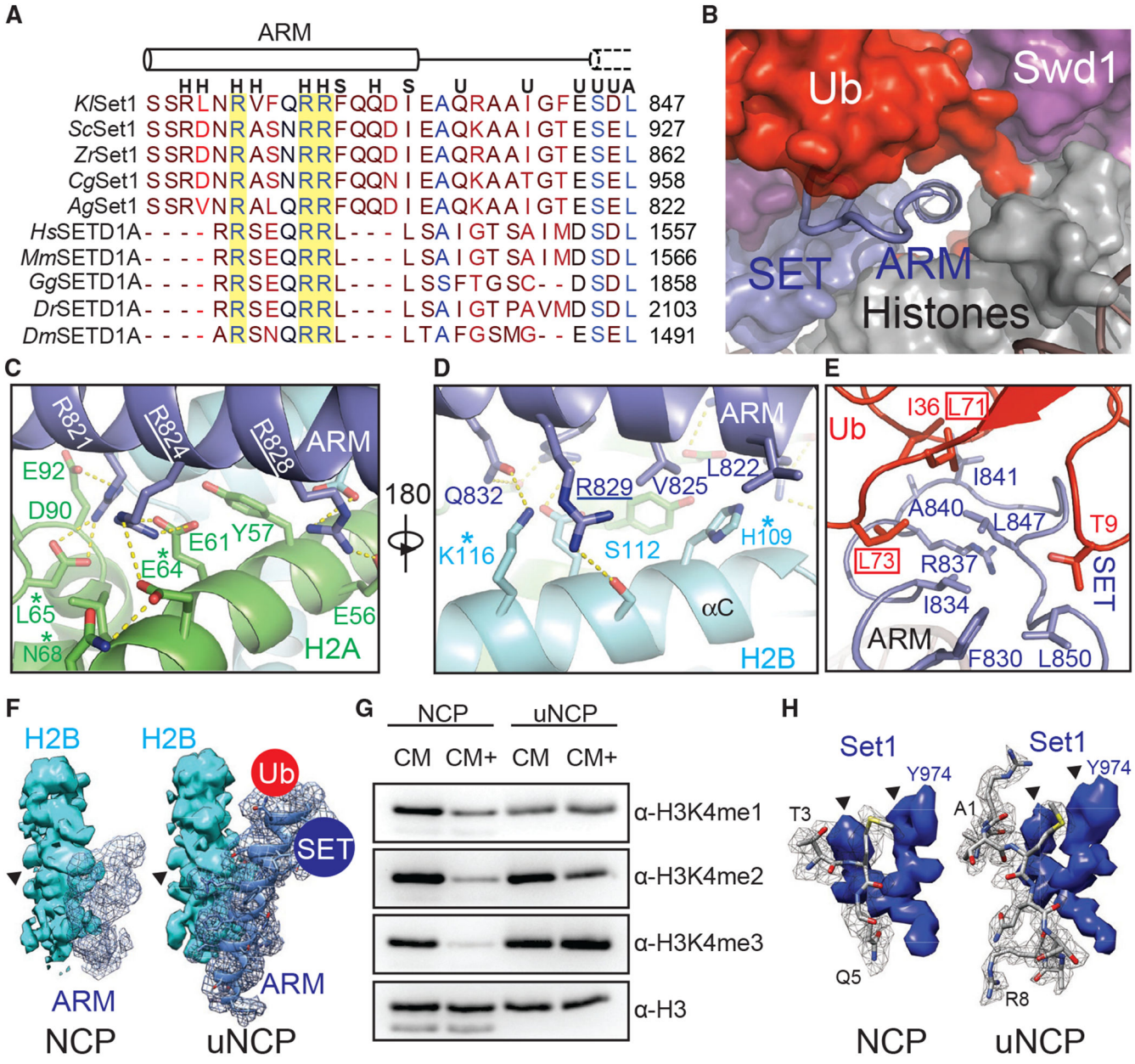

Figure 7. The Set1 ARM Regulates COMPASS H2Bub Sensitivity

(A) Sequence alignment of the nSET ARM across *K. lactis* (*Kl*), *S. cerevisiae* (*Sc*), *Z. rouxii* (*Zr*), *C. glabrata* (*Cg*), *A. gossypii* (*Ag*), *H. sapiens* (*Hs*), *M. musculus* (*Mm*), *G. gallus* (*Gg*), *D. rerio* (*Dr*), and *D. melanogaster* (*Dm*) orthologs. The dotted cylinder represents the unraveled SET N-terminal helix. Cylinders represent helices, and lines indicate coiled structure. The strictly conserved arginine residues are highlighted by a yellow background. Letters above the alignment indicate the interactions the residue is involved in. (H) indicates a histone interaction, (S) indicates a SET domain interaction, (U) indicates a Ub interface, and (A) indicates a Sett ARM interaction.

(B) View of the tunnel formed by the junction between Set1 (blue, surface), Swd1 (magenta, surface), Ub (red, surface), and the histone octamer (gray, surface). Swd3 sits at the

periphery (green, surface). The Set1 ARM helix (blue, cartoon) sits in the center of this tunnel. The loop connecting the SET domain and the ARM helix is shown in tube form.
(C) Close-up view of the Set1 ARM helix (blue) against the acidic surface of H2A (green). Side chains are shown in sticks. Two of the three strictly conserved arginine residues that impair H2Bub-H3K4me crosstalk (Kim et al., 2013) are underlined. H2A residues identified in (Nakanishi et al., 2008) critical for H2Bub-dependent H3K4 methylation are marked by an asterisk. Hydrogen bonds and salt bridges are shown as dashed yellow lines.
(D) Close-up view of the Set1 ARM (blue) against the H2B αC helix (cyan). Side chains are shown in sticks. The third strictly conserved arginine residue involved in the H2Bub-H3K4me crosstalk (Kim et al., 2013) is underlined. H2B residues identified by Nakanishi et al. (2008) to be important for H2Bub-dependent H3K4 methylation are marked by an asterisk. Hydrogen bonds and salt bridges are shown as dashed yellow lines.
(E) Close-up view of the three-way interface between the Set1 (blue) ARM, SET N terminus, and the Ub (red) Ile36 site. Side chains are shown in sticks. The ARM helix packs against the SET N terminus using an interlocking series of hydrophobic amino acids. Ub contributes to this interface by helping form the connecting loop between the ARM and SET regions through hydrophobic packing. Ub Leu71/Leu73, identified by Holt et al. (2015) to be important for H2Bub-stimulated H3K4me activity, are boxed.
(F) Comparison of the Set1 ARM density (blue mesh) between the unmodified NCP-bound (left) and uNCP-bound (right) structure of the COMPASS eCM. The neighboring H2B density (cyan, surface) was used to normalize the ARM densities. The key side-chain feature on H2B used for controlling the map contour level is indicated by a triangle. The uNCP density has the model of the ARM superposed in the mesh. The positions of where Ub and the SET domain dock on the ARM helix are indicated by a red and blue circle, respectively.
(G) H3K4 methyltransferase activity of the COMPASS CM and CM plus (CM+) on NCP and uNCP substrates. CM+ activity is suppressed relaive to the CM on NCPs and regains robust methyltransferase activity on uNCPs.
(H) Comparison of the H3 N-terminal tail density (gray mesh) at the Set1 catalytic cleft between the unmodified NCP-bound (left) and uNCP-bound (right) structure of the COMPASS eCM. The density of a nearby Set1 sequence was used to normalize the H3 N-terminal tail densities. The key features of the Set1 density for controlling the map contour level is indicated by triangles. The models of the H3 N-terminal tail centered at the H3K4 methylation site are shown in sticks.

KEY RESOURCES TABLE

REAGENT or RESOURCE	SOURCE	IDENTIFIER
Antibodies		
Rabbit monoclonal anti-H3K4me1	Cell Signaling Tech	Cat#5326, RRID:AB_10695148
Rabbit polyclonal anti-H3K4me2	Abcam	Cat#ab7766, RRID:AB_2560996
Rabbit polyclonal anti-H3K4me3	Abcam	Cat#ab8580, RRID:AB_306649
Rabbit polyclonal anti-H3	Abcam	Cat#ab1791, RRID:AB_302613
Mouse monoclonal anti-GST	Thermo-Fisher	Cat#MA4-004-HRP, RRID:AB_2537634
Mouse monoclonal anti-His_6	Thermo-Fisher	Cat#MA1-135-HRP, RRID:AB_2610638
Anti-rabbit, HRP-conjugated	GE Healthcare	Cat#NA934
Bacterial and Virus Strains		
E.coli BL21 (DE3)	NEB	C2527I
Chemicals, Peptides, and Recombinant Proteins		
Glutathione Sepharose FF	GE Healthcare	17513201
HiTrap Q-HP, 5mL	GE Healthcare	17115301
Superdex 200 Increase 10/300 GL	GE Healthcare	28990944
S-adenosylmethionine	NEB	B9003S
H3 (K4M)	Colorado State PEP	N/A
H2B (K120C)	Colorado State PEP	N/A
H3	Colorado State PEP	SKU 00042
H2A	Colorado State PEP	SKU 00026
H4	Colorado State PEP	SKU 00068
TEV protease	In house	N/A
Deposited Data		
COMPASS eCM-uNCP complex model coordinates	This paper	PDB: 6UH5
COMPASS eCM-uNCP cryo-EM map	This paper	EMD: 20767
COMPASS eCM-NCP complex model coordinates	This paper	PDB: 6UGM
COMPASS eCM-NCP cryo-EM map	This paper	EMD: 20765
Experimental Models: Cell Lines		
Spodoptera frugiperda: Sf9	Life Technologies	B825-01
Trichoplusia ni: HighFive	Life Technologies	B85502
Recombinant DNA		
pFB-GST-*Kl*Set1	This paper	N/A
pFB-His_6-*Kl*Swd1	This paper	N/A
pFB-*Kl*Swd3	This paper	N/A
pFB-*Kl*Bre2	This paper	N/A
pFB-*Kl*Sdc1	This paper	N/A
pFB-*Kl*Spp1	This paper	N/A
pFB-*Kl*Shg1	This paper	N/A

REAGENT or RESOURCE	SOURCE	IDENTIFIER
pFB-*Kl*Swd2	This paper	N/A
*Xl*H3 (K4M) pET3a	This paper	N/A
*Xl*H2B (K120C) pET3a	This paper	N/A
Ub G76C pET	This paper	N/A
Software and Algorithms		
Phenix	Adams et al., 2010	https://www.phenix-online.org/
Coot	Emsley and Cowtan, 2004	https://www2.mrc-lmb.cam.ac.uk/personal/pemsley/coot/
Pymol	Pymol	https://pymol.org/2/
UCSF Chimera	Pettersen et al., 2004	https://www.cgl.ucsf.edu/chimera/
Relion-3.0	Zivanov et al., 2018	https://www3.mrc-lmb.cam.ac.uk/relion/
cisTEM	Grant et al., 2018	https://cistem.org
GCTF	Zhang, 2016	https://www.mrc-lmb.cam.ac.uk/kzhang/